EXPERIMENTAL AND NUMERICAL ASSESSMENT OF THE ELECTRO-MECHANICAL LIMITS OF Nb_3Sn ACCELERATOR MAGNETS

Presented at CHATS on Applied Superconductivity.
5th May 2023

J. Ferradas Troitino, B. Bordini, A. Devred, P. Ferracin, S. Izquierdo Bermudez, F.J. Mangiarotti, A. Milanese, C. Senatore, E. Todesco and G. Vallone

Outline

3D rendered view of a MQXF short model magnet, whose analysis is treated in the slides.

- Introduction / motivation
- Methodology
- Results at the strand level
- Results at the magnet level
- Comparison
- Conclusions

Jose Ferradas Troitino
3rd May 2023

Outline

3D rendered view of a MQXF short model magnet, whose analysis is treated in the slides.

- Introduction / motivation
- Methodology
- Results at the strand level
- Results at the magnet level
- Comparison
- Conclusions

Jose Ferradas Troitino
3rd May 2023

Nb_3Sn accelerator magnets

On the search for higher magnetic fields in accelerator magnets

Presently, Nb_3Sn superconductors are the preferred solution for the windings of high-field accelerator magnets:

- Performance above Nb-Ti limits.
- Proven large-scale industrial production.

State-of-the-art Nb_3Sn wires surpass the values of J_c **> 1000 A/mm²** (SC area) **at 16 T and 4.2 K.**

Nb_3Sn Rutherford cable. Source: [CERN]

However, these appealing properties are impaired by:

The strain sensitivity and **brittle** nature of the superconductor.

The determination of sound electro-mechanical limits for Nb_3Sn technology becomes of paramount importance!

High-field accelerator units

$$\vec{f} = \vec{J} \times \vec{B}$$

Magnets are intrinsically characterized by the large electro-magnetic forces arising from the combination of the required high current densities, J, and produced magnetic fields, B.

A bit of history and motivation for our work

During the past years, our community has tried to shed some light on the electro-mechanical properties of Nb_3Sn superconductors.

- To establish safe strain/stress limits for operation.

- Developing the necessary mathematical background to describe the strain effects on the superconducting properties.

Laboratory-scale experiments

Exploring the electro-mechanical response of single wires, up to full cables, when subjected to mechanical loads.

- Back in the 1980's by Ekin and co-workers [1] – [2]
- **University of Geneva** **[3] – [11]**
- **CERN** **[12] – [16]**
- University of Twente [17] – [18]
- NHMFL [19] – [21]
- Fermilab [22] – [24]

Direct assessment on magnet configuration

Magnet performance studied as a function of different conductor stress levels.

- Lawrence Berkeley National Lab. (LBNL)
  TQ magnet
  [25]

- CERN
  SMC magnet
  [26 - 27]
  MQXF magnet
  [28]

Overview on Nb_3Sn

- Strain sensitive and **brittle** superconductor

Strain → Deformation of the crystal structure → Change in the phonon spectrum and the electronic bands → Change in superconducting properties (T_c and B_{c2}), and thus, critical current!

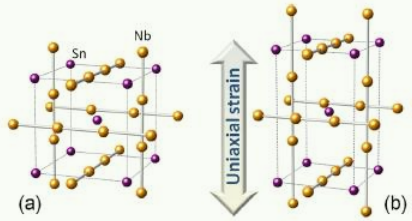

G. De Marzi et al. arXiv:1210.3705, 2012.

1

Brittle fracture of the superconducting phase → Reduction of the current-carrying surface → Reduction in conductor performance / critical current!

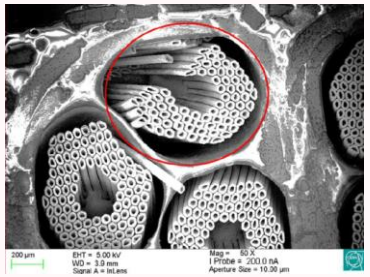

A. Moros et al., IEE TAS 2023

2

Overview on Nb_3Sn

Critical surface → ***Exponential scaling law proposed by Bordini, Bottura et al. [29] – [30]***

Initially postulated to predict the effects of mechanical strain in axially loaded [illegible] strain region!

I_1 - first invar[illegible] incipal

For magnet design, instrumental to apply our understanding acquired at the conductor level.

- Are conductor tests applicable to magnet configuration?
- Can we provide reliable limits for the technology?

Based on experimental results and numerical modelling, we will try to provide answers to these fundamental questions **at the magnet scale.**

1

- *Transversally* [illegible] *validated in:*

- *2D and 3D detailed* [illegible]
  [31]-[32] Bordini, Catt[illegible]ani, Baffari et al.
  [5] Senatore, Bagni, Calzolaio et al.
  [33] Chiesa, Wang et al.

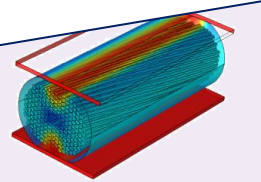

Cattabiani, Baffari et al.

- *Transversally loaded cable stacks (**macro-scale model**)*

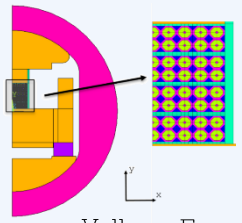

[34] – [35] *G. Vallone et al.*

It can be applied to a 2D magnet cross-section (already published).

Vallone, Ferracin, Bordini et al.

Outline

3D rendered view of a MQXF short model magnet, whose analysis is treated in the slides.

Jose Ferradas Troitino
3rd May 2023

- Introduction / motivation
- Methodology
- Results at the strand level
- Results at the magnet level
- Comparison
- Conclusions

Methodology

- Domain homogenized down to an octagonal strand representation (Cu, Nb_3Sn).
- 2D static structural analysis. Material properties from literature. Described in details in [34] – [35].
- Boundary conditions play a critical role. Plane stress used in the simulations shown in these slides.

- The strand critical current is computed averaging the critical current over the strand area (perfect current redistribution within the strand).
- The horizontal and vertical strain in the Nb_3Sn area are amplified with a constant factor:

$$\varepsilon_i \rightarrow \alpha\, \varepsilon_i$$

Amplification when scaling the model to the filament level (strand-to-filament amplification factor).

- Furthermore, the approach considers the effect of the thermal contraction mismatch on strand constituents (from the reaction to cryogenic temperatures). This "pre-compression strain tensor" is added to the one computed by the mechanical model:

$$\begin{aligned} \varepsilon_{zz} &= \varepsilon'_{zz} + \varepsilon_{l0} \\ \varepsilon_{xx} &= \varepsilon'_{xx} - \upsilon\varepsilon_{l0} \\ \varepsilon_{yy} &= \varepsilon'_{yy} - \upsilon\varepsilon_{l0} \end{aligned}$$

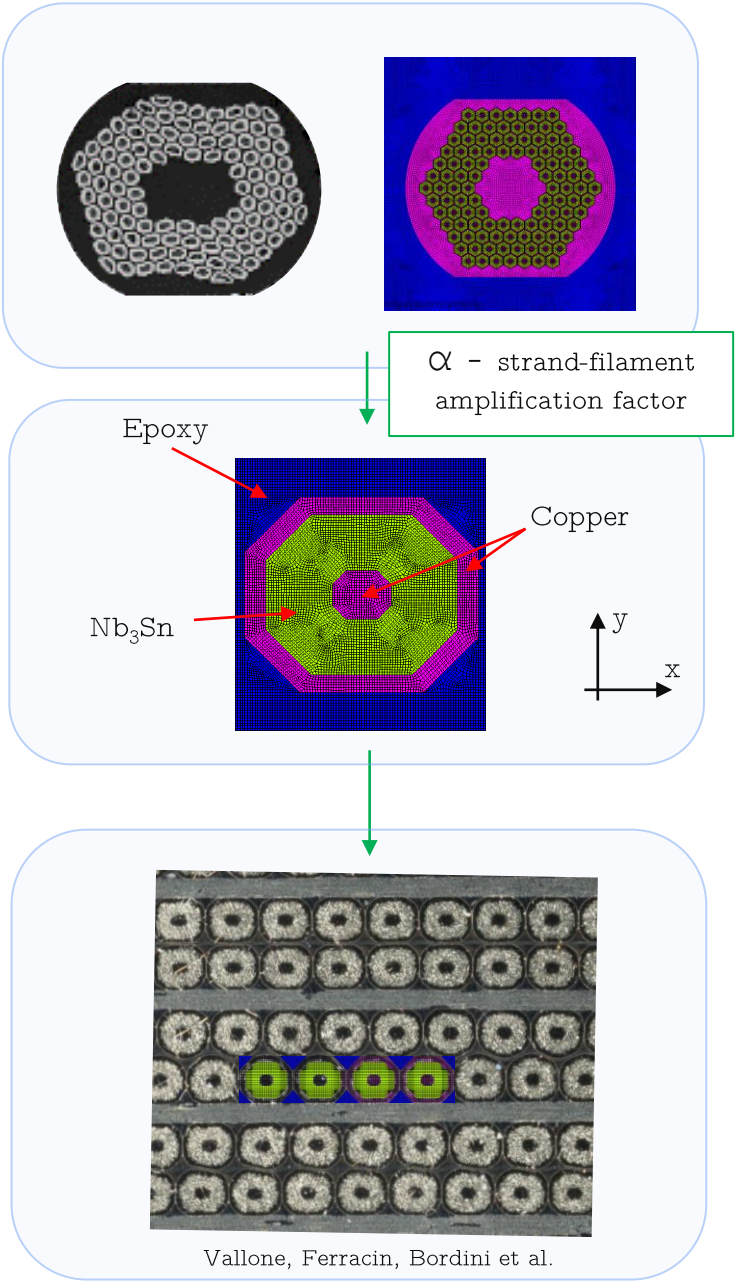

Methodology

- The following fitting parameters are needed to feed the scaling law:
  - Non-strain related: C_0, B_{c2} (0,0), T_c (0)
  - Strain related: C_1, ε_{l0}

Requirement: Characterization of the desired strand using a standard WASP measurement.

- **Recall:** This approach is valid when the mechanism governing the Ic change is a modification on the strain state of the superconducting phase:
  - Elastic (recovered when the load is removed)
  - Plastic (mainly coming from matrix plasticization)

- A failure criteria is needed (separately) to deal with the brittle fracture of the Nb_3Sn phase.
  - Proposal from Vallone et al. in https://indico.cern.ch/event/1177999/
  - **Indications of clear differences depending on the test configuration (4-wall fully supported strand, 2-wall)**
  - Not covered in these slides!

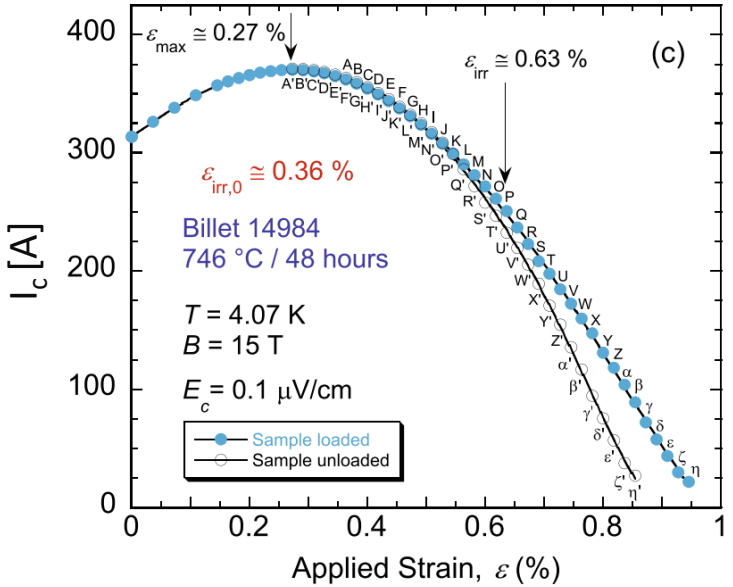

Plot from N. Cheggour et al. Scientific Reports (2019)

Outline

3D rendered view of a MQXF short model magnet, whose analysis is treated in the slides.

Jose Ferradas Troitino
3rd May 2023

- Introduction / motivation
- Methodology
- Results at the strand level
- Results at the magnet level
- Comparison
- Conclusions

Ic vs. transverse stress on single wires

UNIVERSITÉ DE GENÈVE

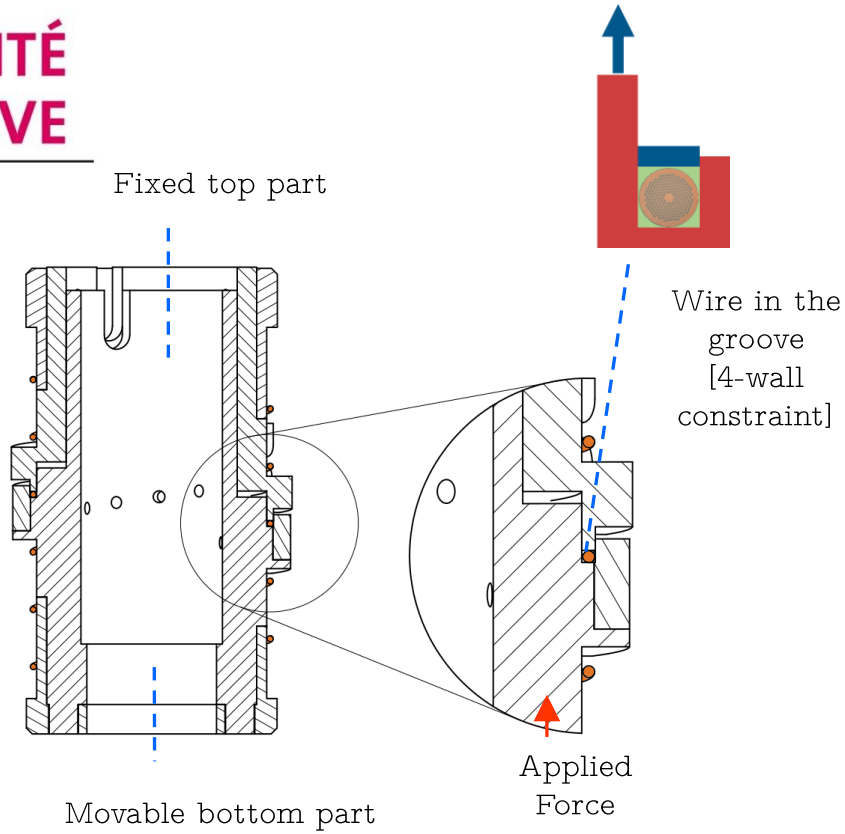

C-WASP – I_c vs transverse stress measurements

Trying to reproduce the operating conditions of accelerator magnets.

Example on measurement results

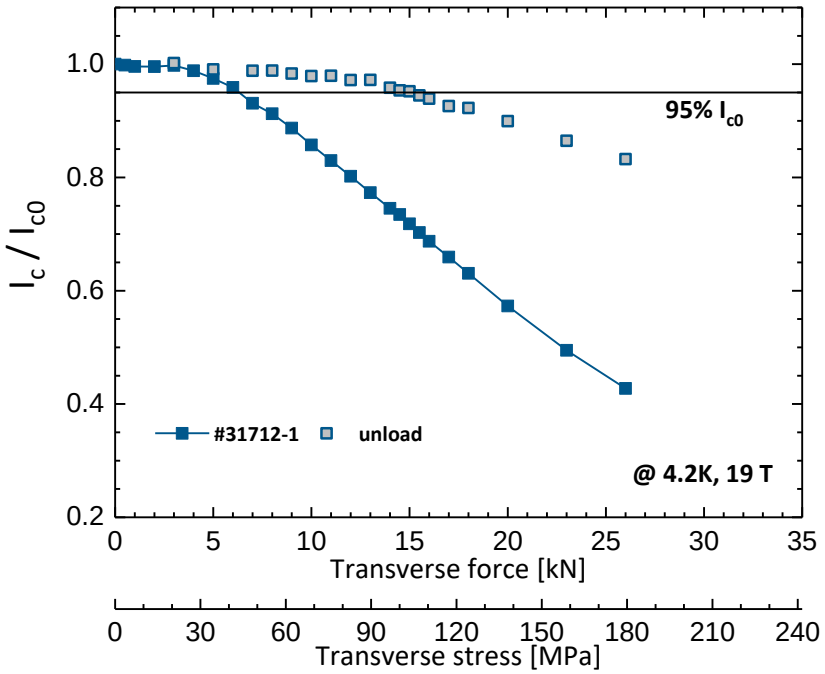

To compare results among wires, a conventional irreversible threshold is generally defined as the stress level leading to a permanent 5% loss of Ic.

Plot shows results at 19 T.

Ic vs. transverse stress on single wires

UNIVERSITÉ DE GENÈVE

Fitting parameters extracted from Ic vs axial strain measurements.

Amplification factor assessment:

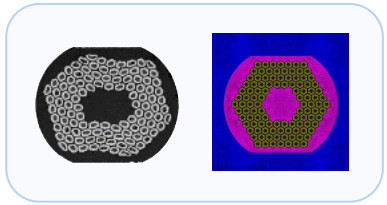

$\alpha_{RRP} = 1.2$

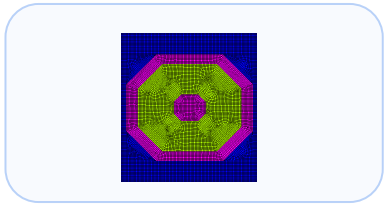

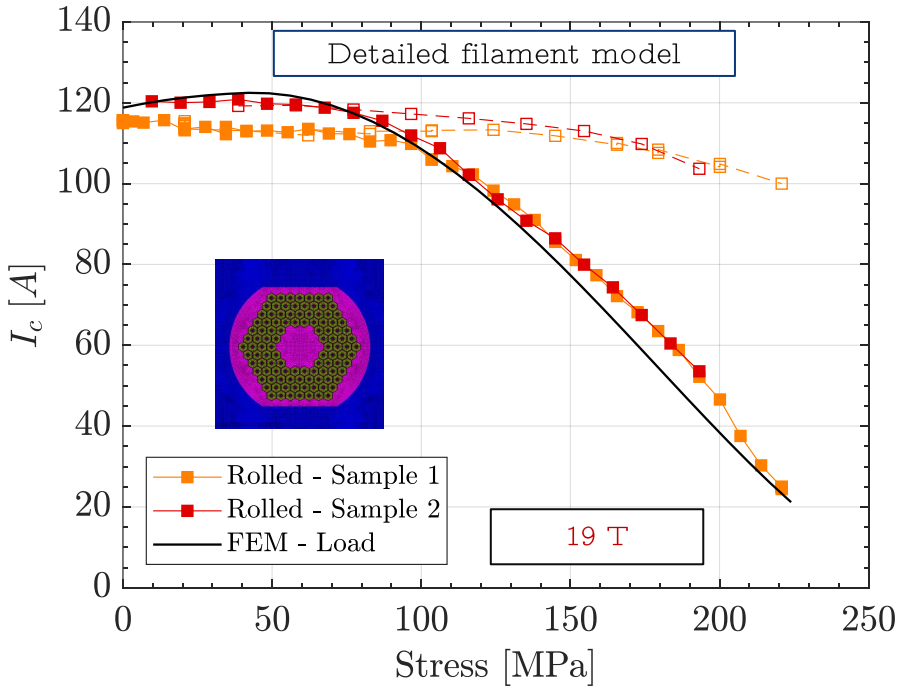

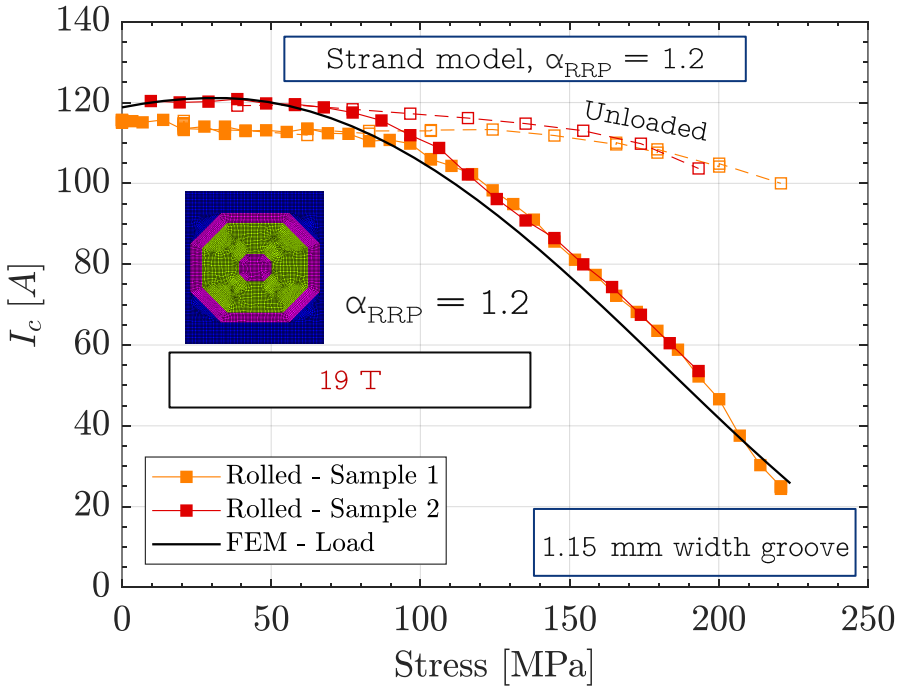

0.85 mm RRP 108/127 15% rolled (HL-LHC MQXF quadrupole)

Ic vs. transverse stress on single wires

UNIVERSITÉ DE GENÈVE

Fitting parameters extracted from Ic vs axial strain measurements.

Simulation and experimental results:

0.85 mm RRP 108/127 15% rolled (HL-LHC MQXF quadrupole)

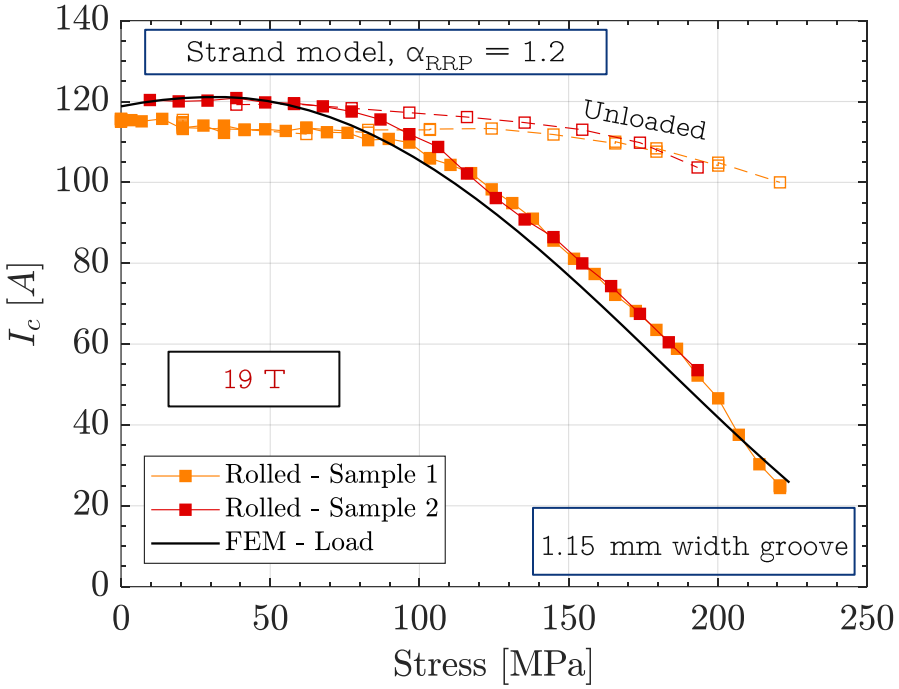

1 mm PIT 192 15% rolled (FRESCA2 dipole)

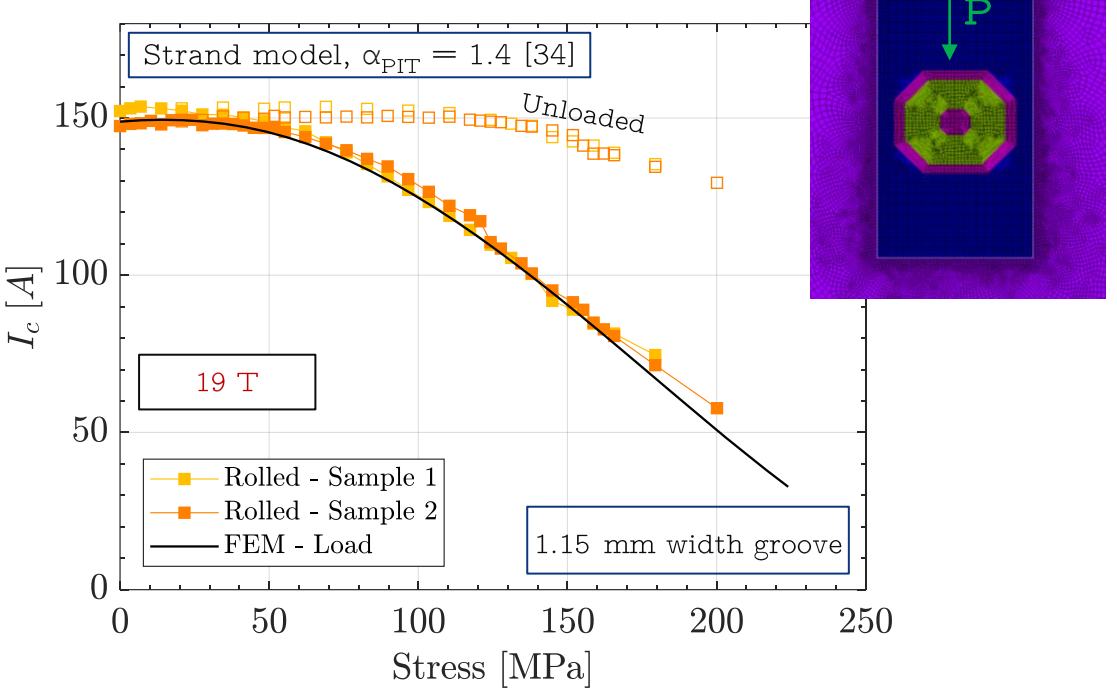

- Model catches the Ic reduction when the transverse load is applied for both wire technologies.
  $\alpha_{PIT} = 1.4$, consistent with cable model [34] → calculated by direct fitting of experimental data. Larger strain sensitivity than RRP (core, etc [32]).
- Simulation results after force unload are inferred using the experimental data. Model is not predictive, but it can still provide $I_{c\ unload}$ when coupled to a C-WASP measurement (additional slides). Development on-going.

Ic vs. transverse stress on single wires

UNIVERSITÉ DE GENÈVE

Fitting parameters extracted from Ic vs axial strain measurements.

Simulation and experimental results:

0.85 mm RRP 108/127 15% rolled
(HL-LHC MQXF quadrupole)

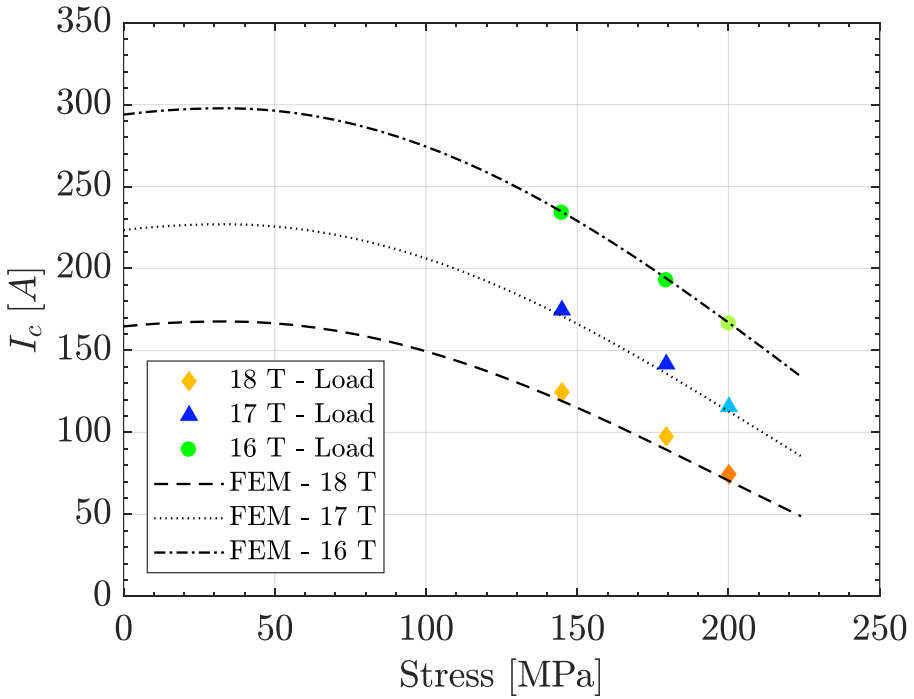

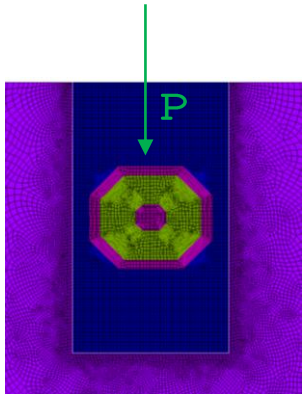

Model validated using the complete magnetic field range available experimentally.

Wrap up on tests on single wires

Important information for magnet application:

- As already shown by previously published models, the exponential scaling law is able to correctly describe the reduction in Ic due to applied transverse stresses as high as 200 MPa.

Indication that the dominating mechanism is the strain effect on B_{c2} and T_c

For this test configuration (4-wall)!

- Independent confirmation on three different wire types has been recently published by Senatore et al. [11] - detailed analysis of the experimental $B_{c2}(\varepsilon)$ evolution.

RRP up to ~ 250 MPa (anvil applied normal stress)

PIT up to ~ 200 MPa (anvil applied normal stress)

- Post-mortem inspection of C-WASP test samples revealed the absence of transversal cracks sectioning the Nb_3Sn filaments [8] – [10].

- Finally, consistent results found on PIT **cable** tests, where the onset of cracks was identified at around 180 – 200 MPa [12] – [14].

Bladder and key set-up.

The behavior can be successfully reproduced using the scaling law (already shown by previous studies). This time, also with a simplified strand representation!

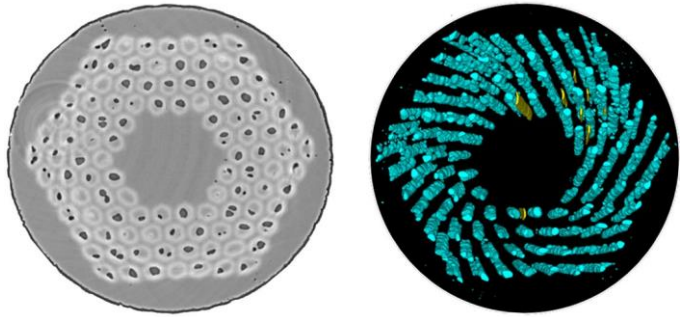

Bagni, et al. SUST - 2022

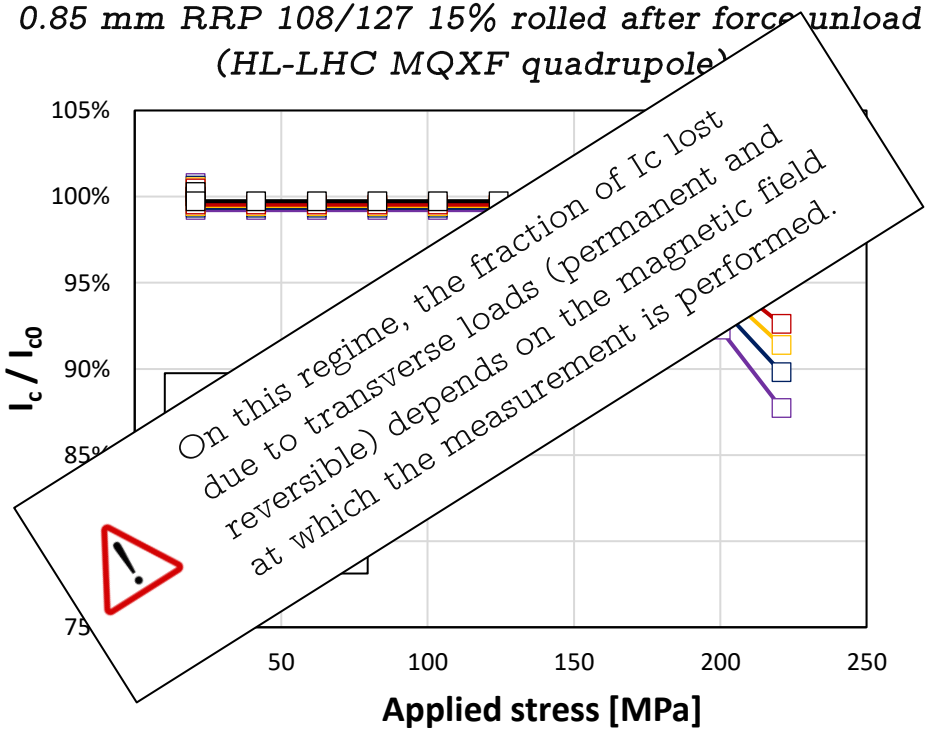

Outline

3D rendered view of a MQXF short model magnet, whose analysis is treated in the slides.

- Introduction / motivation
- Methodology
- Results at the strand level
- Results at the magnet level
- Comparison
- Conclusions

Jose Ferradas Troitino
3rd May 2023

Electro-mechanical limits on magnet configuration

HL-LHC MQXF project:

One short model magnets is being used to explore the electro-mechanical limits of the conductor in magnet configuration.

- MQXFS7 – 2 coils with PIT and 2 coils RRP conductor.

- Magnet pre-load gradually increased searching for signs of performance reduction. Similar test as the one reported by H. Felice et al. [25].

- **Pre-load** level at cold **estimated** using mechanical **instrumentation** placed on the **winding pole** (representative of stress in inner radius pole turn conductor, standard FE model).

Instrumentation on the **winding pole (indirect assessment of coil stress)**

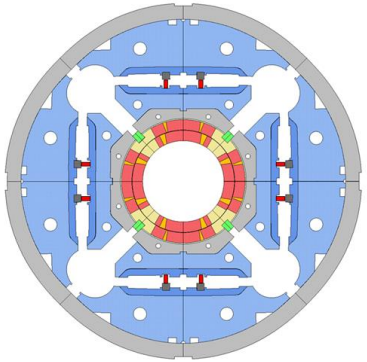

Coil pre-load / pre-compression applied by a system of interference keys.

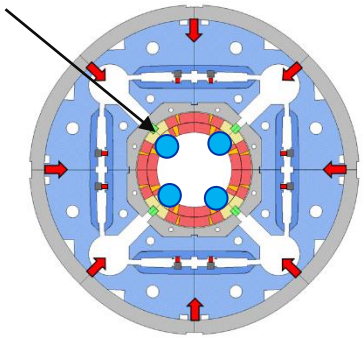

Coil pre-load / pre-compression further increased at cryogenic temperature thanks to the larger thermal contraction of the outer Al-cylinder.

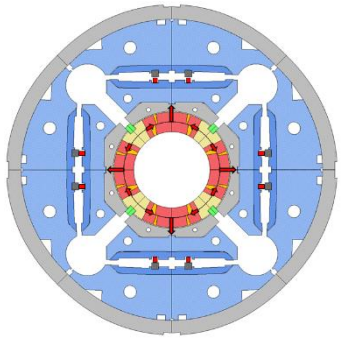

The pre-load counteracts the effect of the e.m. forces during magnet energization.

Reference pre-load. Standard FE model

Coil azimuthal / transverse stress

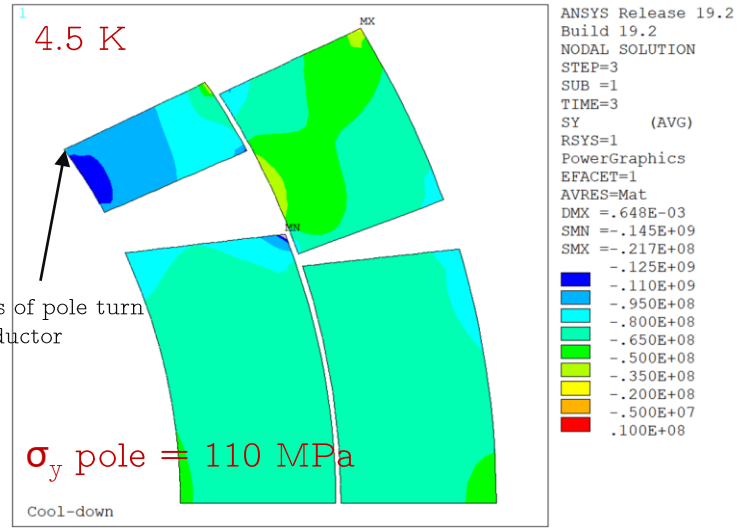

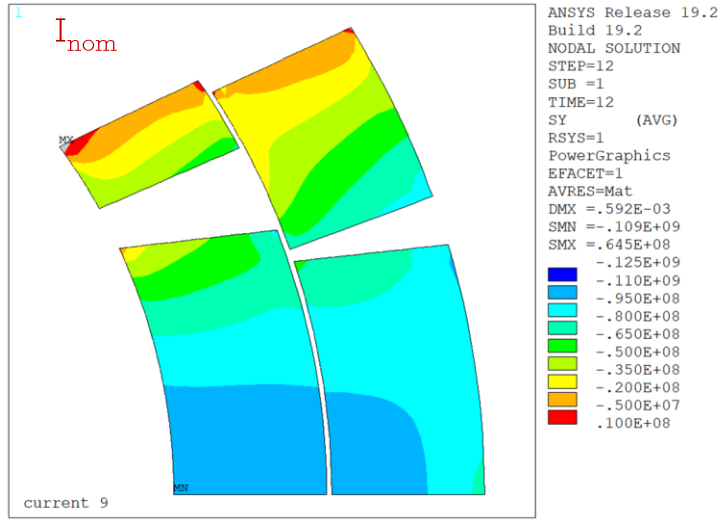

Electro-mechanical limits on magnet configuration

Results on MQXFS7 experiment so-far:

- Critical current characterization on extracted strands for each coil. Coil 211 (PIT) being the limiting coil according to these measurements.

- At 4.5 K, the magnet quenches consistently in the inner layer pole turn of coil 211.
  - Peak field, low stress during powering
  - Close to the peak stress region at cryogenic temperature

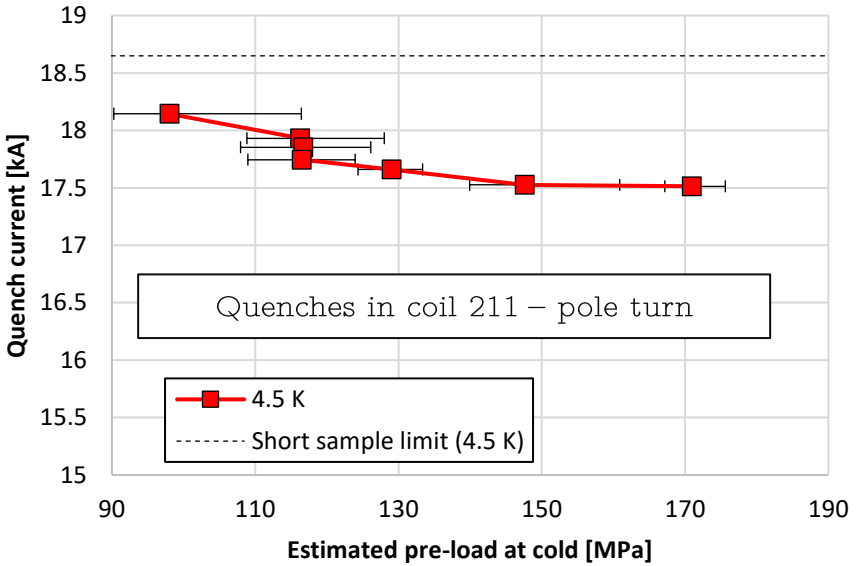

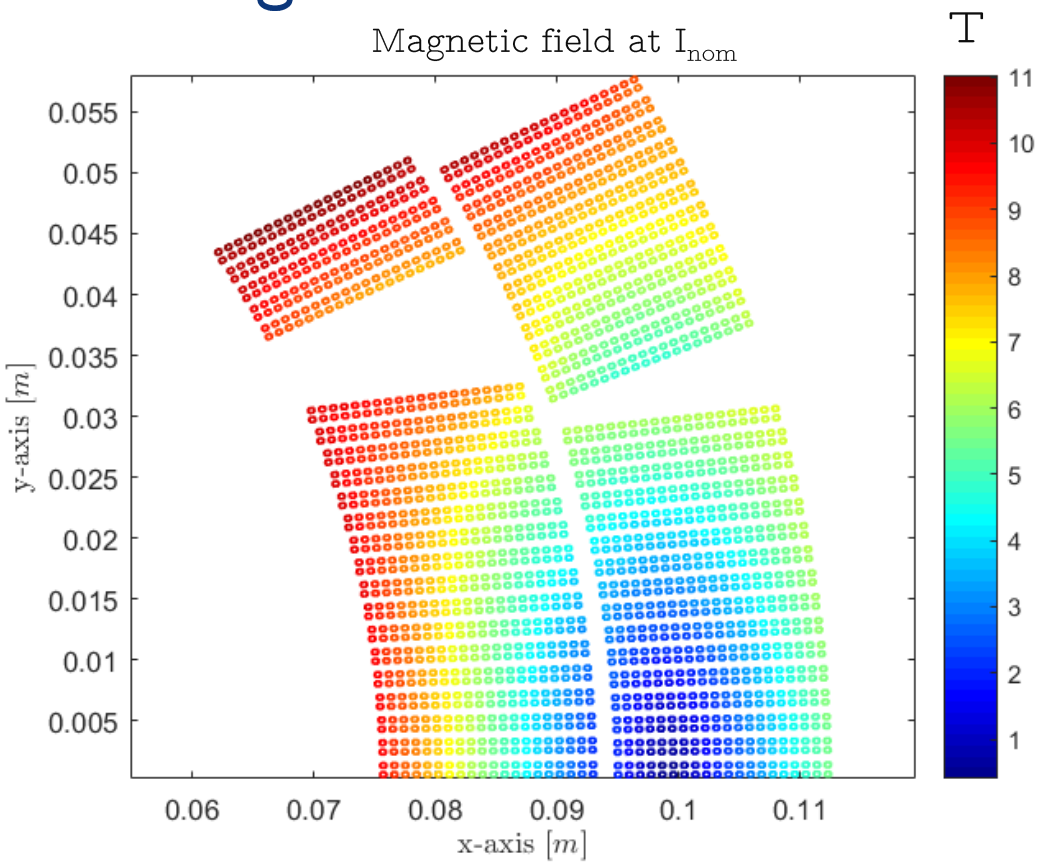

Small decrease in quench current from 100 MPa (97% of SS) to 150 MPa (94% of SS), more assembly iterations to come!

Electro-mechanical limits on magnet configuration

Simulation set-up:

- MQXFS7 experiment modelled using our proposed methodology. Model validated mechanically in [35]. Recall: material properties from literature.
- Strain related fitting parameters (including expected Ic decrease due to permanent strain effects): extracted from available measurements at UNIGE, 1 mm PIT192 strand (**not exactly the same**). Non-strain related: coil extracted strands.
- For each assembly iteration, the pre-load is adjusted to match the experimental results (**we match** the **indirect measurements** at the **winding pole**).
- Quench current defined as the point where the critical surface is crossed.

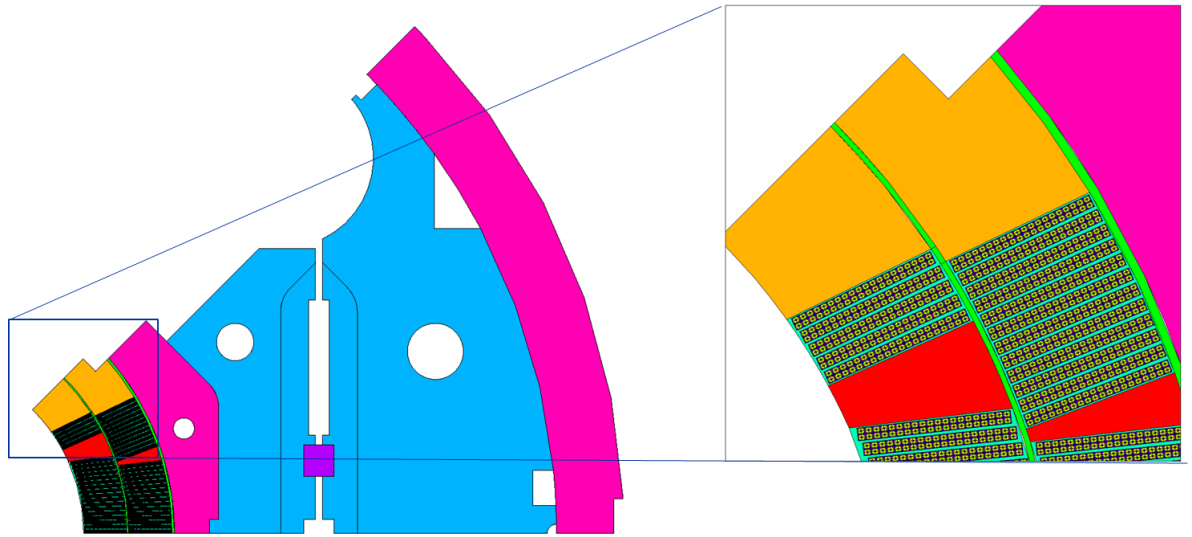

Reference pre-load (Nb$_3$Sn region)

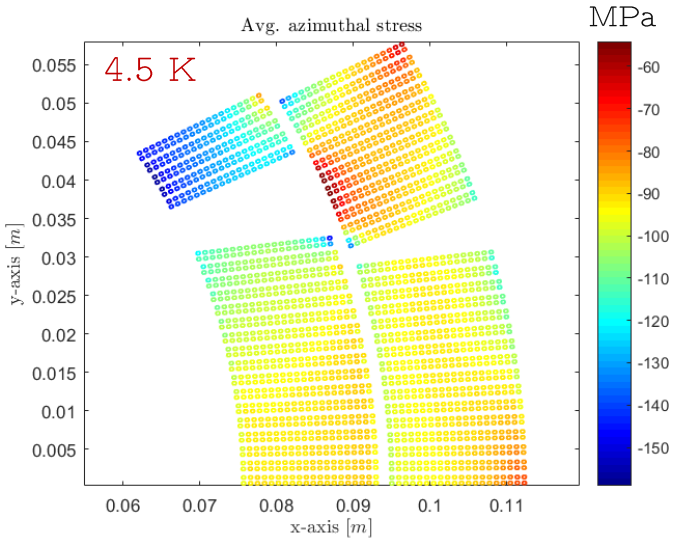

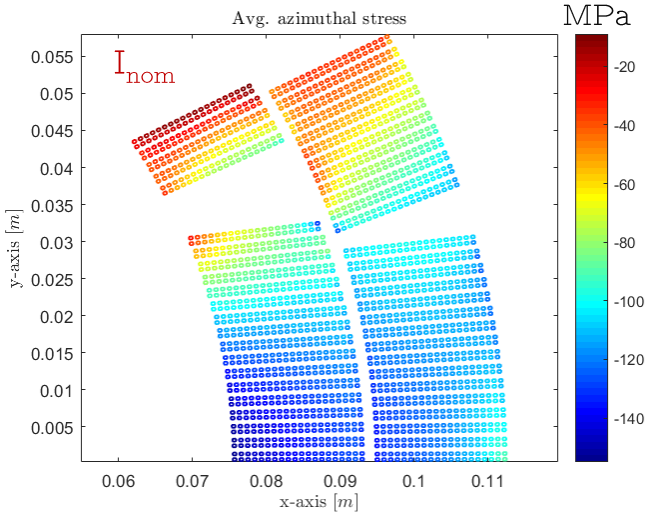

Electro-mechanical limits on magnet configuration

Results:

***Reference pre-load** (4.5 K /110 MPa)*

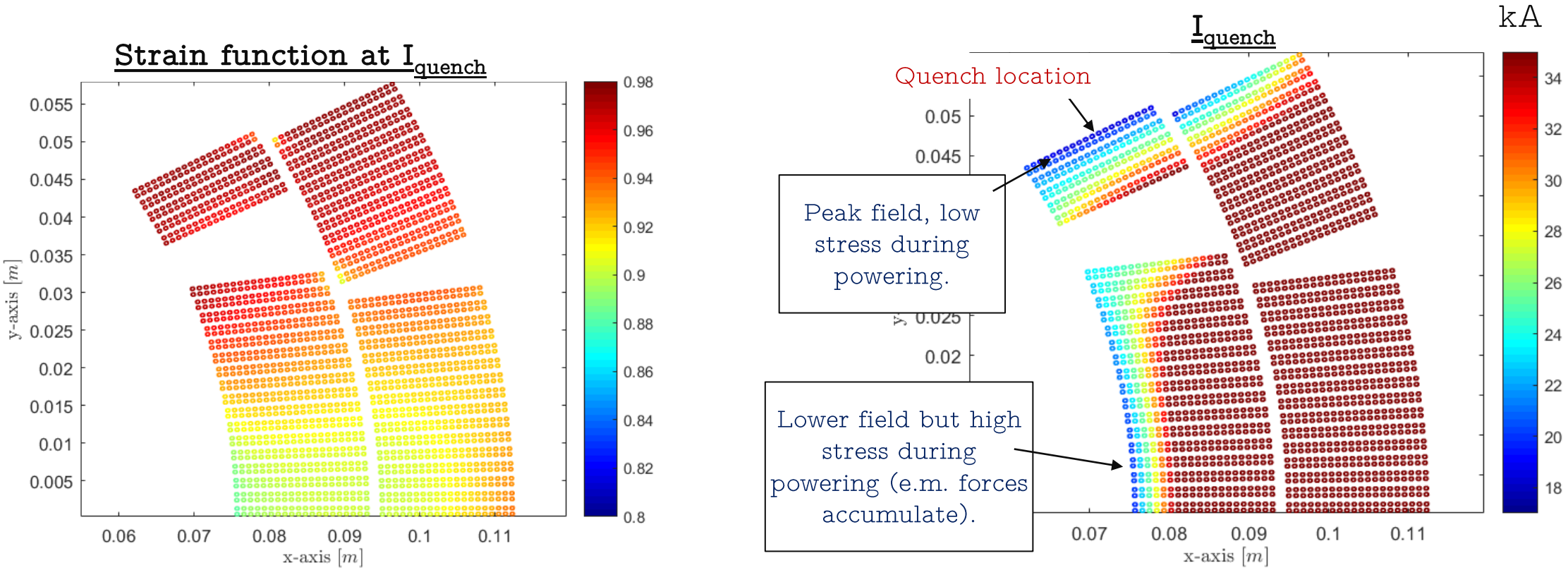

Following the magnet design, the peak field region during powering is found in the pole turn block, which unloads under the action of the electro-magnetic forces. Peak field and highest stress area during powering disentangled!

$$B_{p\ mid\text{-}plane\ (high\ stress)} / B_{p\ pole\ turn\ (low\ stress)} = 0.86$$

$$At\ I_{nominal} \rightarrow B_{p\ mid\text{-}plane\ (high\ stress)} - B_{p\ pole\ turn\ (low\ stress)} \sim 1.5\ T$$

Electro-mechanical limits on magnet configuration

Results:

200 MPa pre-load (4.5 K)

Strain function at I_{quench}

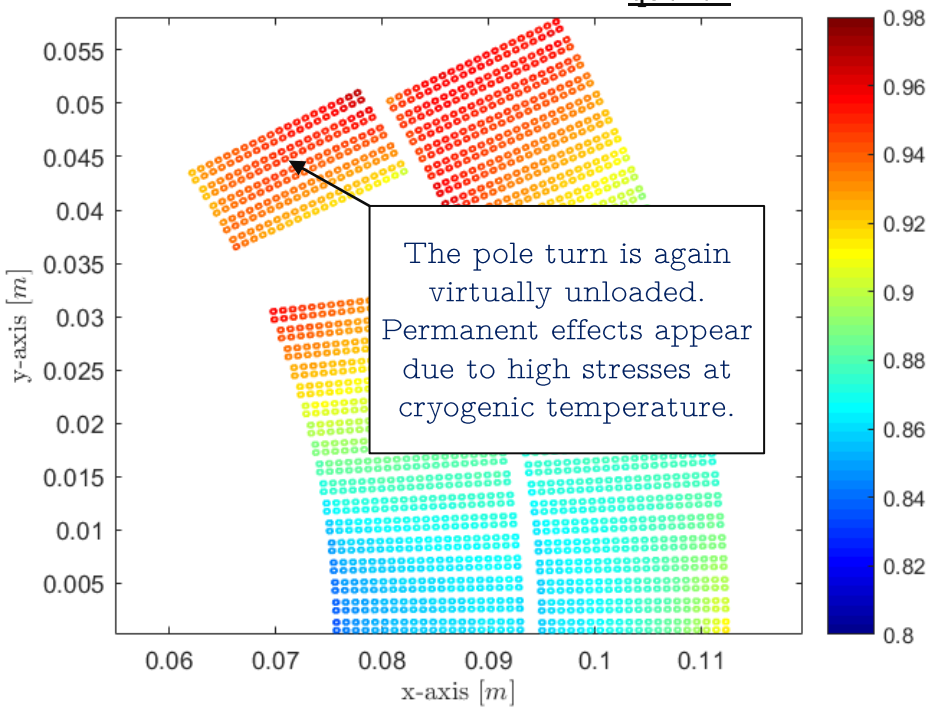

I_{quench} kA

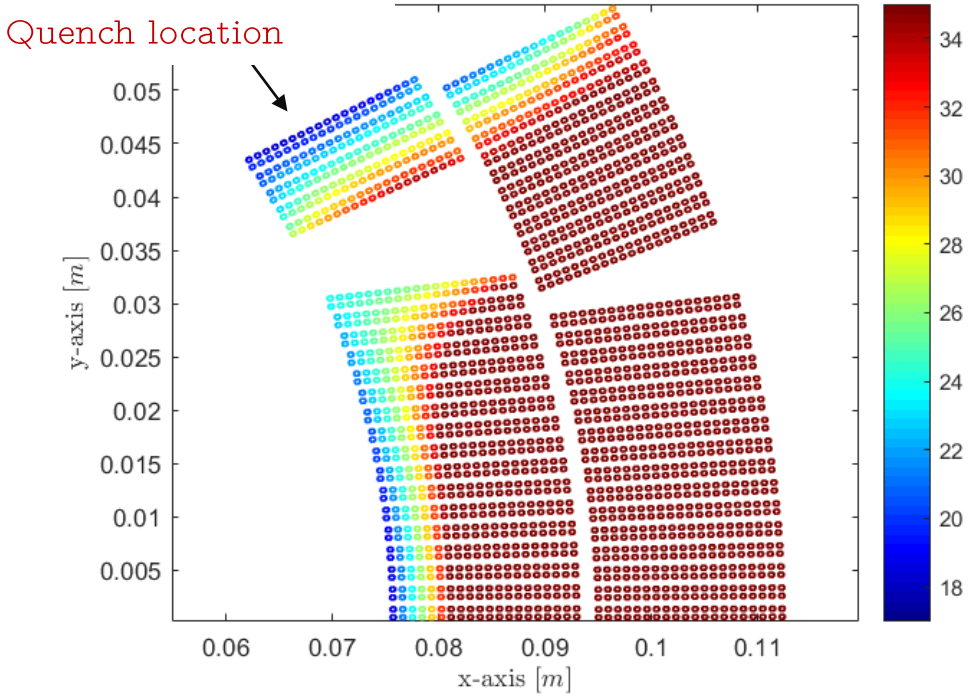

In this particular case for MQXF (4.5 K and strand characteristics), when the magnet is "pre-loaded to the extreme" (200 MPa), a reduction of the short sample limit still appears in the pole turn block due to permanent effects originated by large stresses after cool-down. We do not "jump" to the high stress region (lower field).

Electro-mechanical limits on magnet configuration

Results:

- The magnet strand model (fed with the data from transverse compressive strand tests) shows a similar tendency than the (so-far) measured reduction in quench current.
  - Note that our input data is not strictly the one for the MQXFS7 strand.
  - Experimental and simulated reduction in the same order of magnitude (< 5 %).

- Disregarding the absolute value of I_{quench}/ I_0 → Quench happens in the peak field pole turn conductor, which is unloaded during magnet ramping. Same **result predicted** by the **model**.
- The small short sample reduction with increasing magnet pre-load in this case is thus due to permanent effects arising from the large stress levels at cold in that region.
  - From conductor tests: reduction in Ic under "unloaded conditions" is significantly smaller than in the loaded regime → decrease in quench current contained within 5 % even at high pre-load levels.

- Note that in the real system, geometrical tolerances/imperfections, can modify the conductor strain state. These cases can be simulated as well, but presented results correspond to a perfect geometry.

Measured and computed reduction in quench current.

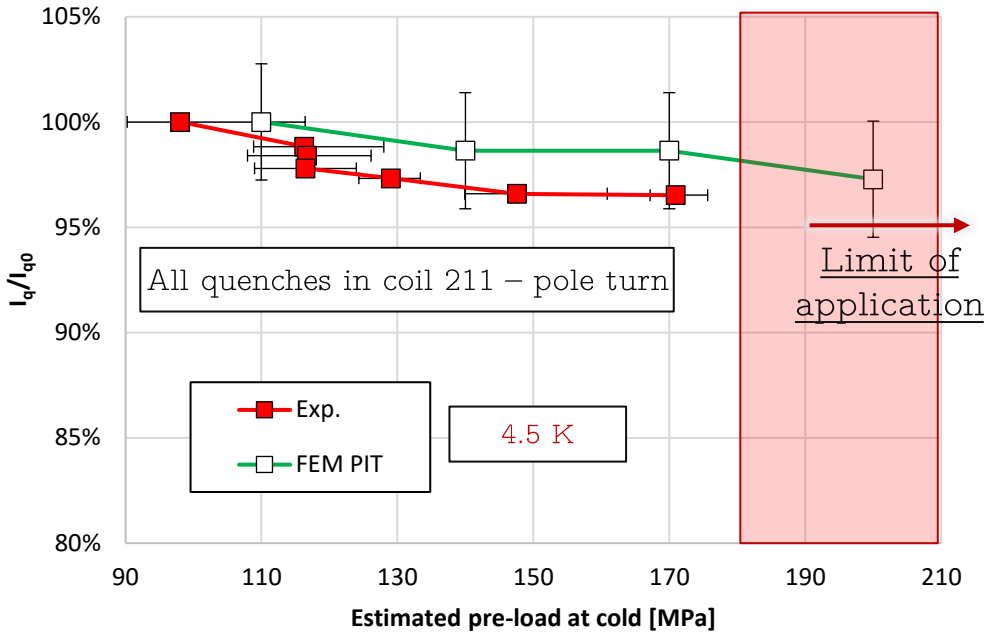

Outline

3D rendered view of a MQXF short model magnet, whose analysis is treated in the slides.

Jose Ferradas Troitino
3rd May 2023

- Introduction / motivation
- Methodology
- Results at the strand level
- Results at the magnet level
- Comparison
- Conclusions

Correlation between strand and magnet results

Correlation between both experiments:

- Methodology allows to compute the magnet limiting current thanks to the inclusion of strain effects on the conductor critical surface (assuming no cracks on the Nb_3Sn region).

Let's focus on the simulated case at 200 MPa (in the limit of validity, based on our current conductor understanding)

Note that: Load line margin is usually 1/3 of the corresponding critical surface one.

- No C-WASP tests are available for the 0.85 mm MQXF PIT strand, but this particular case can be simulated.

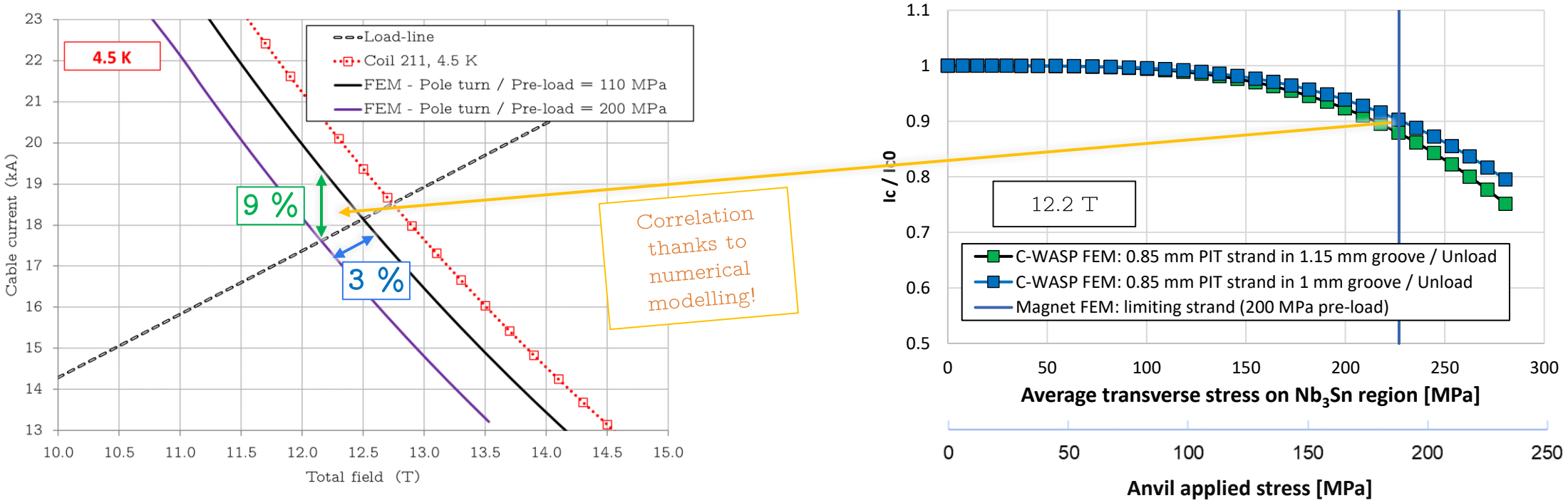

Outline

3D rendered view of a MQXF short model magnet, whose analysis is treated in the slides.

- Introduction / motivation
- Methodology
- Results at the strand level
- Results at the magnet level
- Comparison
- Conclusions

Jose Ferradas Troitino
3rd May 2023

Conclusions

- The accurate reproduction of the strain effects in the Nb_3Sn critical surface (pure strain effects, no cracks) is today a well-known domain of study. A three-dimensional mathematical description is available in the form of the exponential scaling law.
    - The latter has been successfully applied to detailed 2D and 3D FE models, matching experimental data at the conductor level.
- Meaningful results at the conductor scale (cable and strand/wire) can be obtained as well with a simplified geometry of the domain. This reduces significantly the computational cost and allows the application of the scaling law at the magnet scale.
    - Amplification factor needed to go from the strand to the filament level. This factor has been obtained by combining detailed and simplified geometry models. Consistent results with the one obtained by direct fitting of experimental data.
- Under certain support / boundary conditions Nb_3Sn conductors can withstand large stress levels (up to / above 200 MPa), in the absence of cracks sectioning the superconductor. Proven experimentally (B_{c2} evolution, post-mortem inspection) and numerically in wire and cable configuration.
    - In such a regime, the strain sensitivity is strongly magnetic field dependent. It is crucial to consider this dependency for the correct interpretation of test results.
- The direct application of the strand model to the magnet allows to include the strain effects modifying the short sample limit (again, no cracks regime). Good agreement between the obtained simulation results and recent experiment in MQXFS7.
    - Small loss (< 5 %) in magnet quench current even up to high pre-load levels (170 MPa measured in the winding pole).
    - Quench location corresponds to the pole turn block (peak field, low stress during magnet ramping). Caught by the model.
    - Since results are caught by the scaling law (up to this level) → indirect indication that the magnet support conditions are coherent with the conductor tests (C-WASP, FRESCA sample holder). More work on-going to substantiate/support this statement!
- The methodology provides important information to magnet designers. Always interesting to disentangle the peak field and high stress regions. Strand model provides the essential information on where the magnet is limited (peak field-low stress vs. lower field-high stress).
    - From conductor tests, the loss in Ic is significantly smaller when the sample is unloaded (permanent effects: copper plasticization).
    - Design / assembly parameters can be optimized to stay as much as possible in this domain.

Thank you very much for your attention!

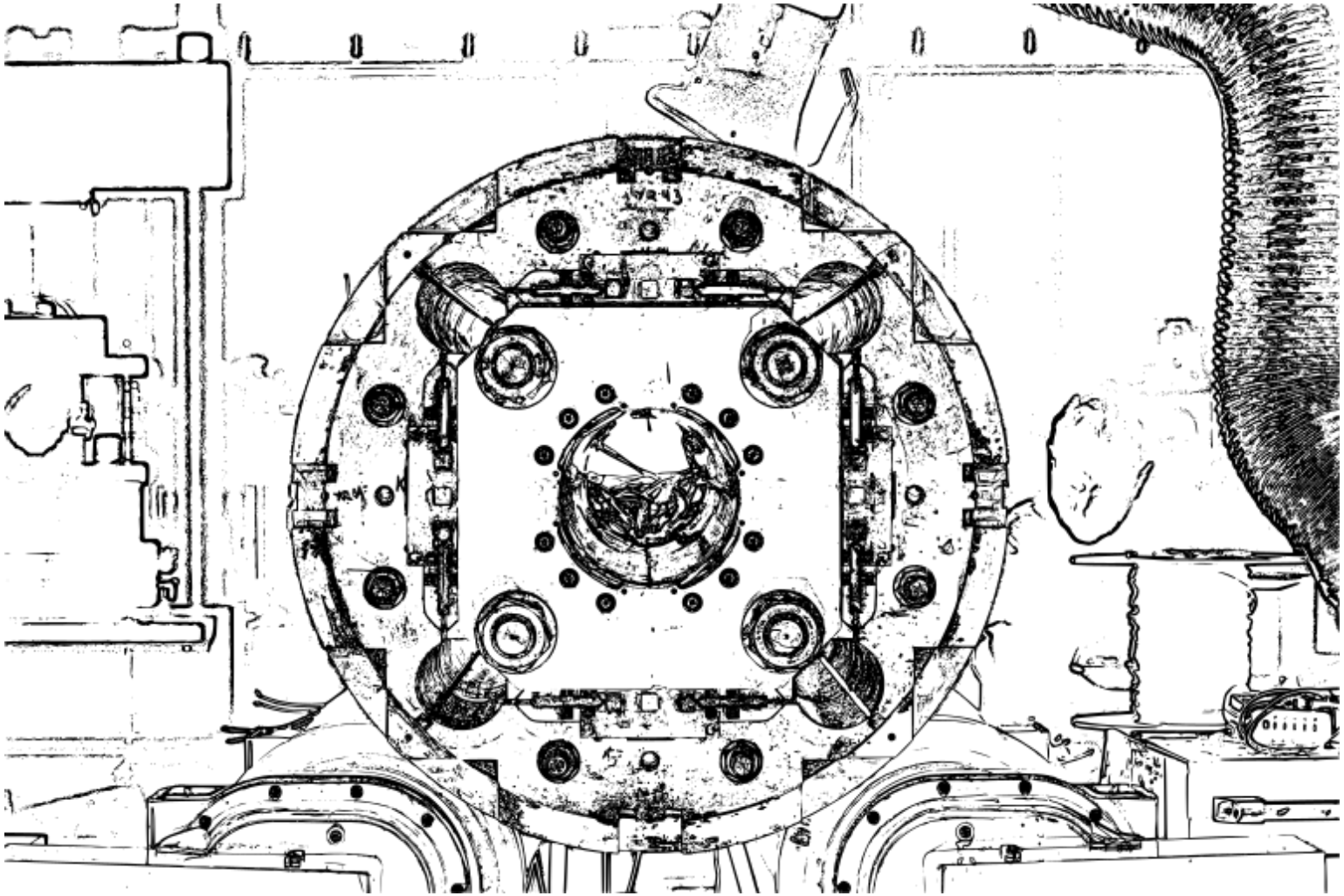

Special thanks (and credits!) to everybody involved:

Susana Izquierdo
Giorgio Vallone
Bernardo Bordini
Tommaso Bagni
Carmine Senatore
Paolo Ferracin

ANNEX

The scaling law

Important to recognize the three-dimensional nature of the scaling law.

It has been proven that for (1) the scaling law can be used under more complex loading conditions.

Focus on transverse loads, those usually of largest magnitude on accelerator magnets

Studies employ Finite Element models to extract the strain tensor. Validated in:

- *Transversally loaded wires (micro-scale models)*

- *2D and 3D models computing I_c*
- *Detailed sub-element geometry*
  - *[31]-[32] Bordini, Cattabiani, Baffari et al.*
  - *[5] Senatore, Bagni, Calzolaio et al.*
  - *[33] Chiesa, Wang et al.*

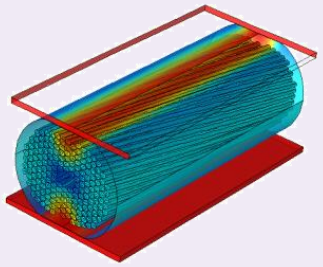

Cattabiani, Baffari et al.

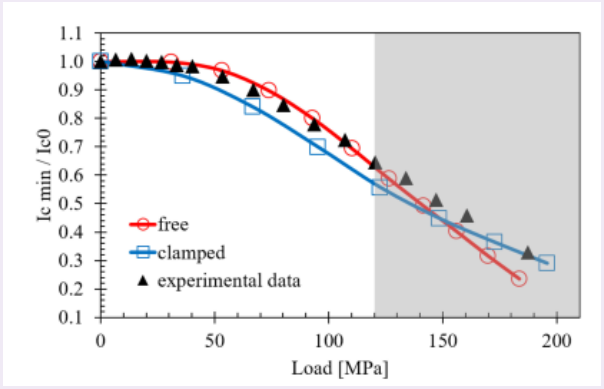

Cattabiani, Baffari et al.

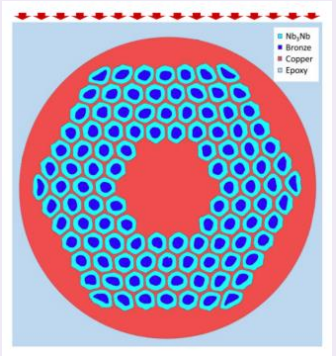

Bagni, Calzolaio et al.

- *Transversally loaded cable stacks (**macro-scale model**)*

[34] – [35] *G. Vallone et al.*

It can be applied to a 2D magnet cross-section (already published).

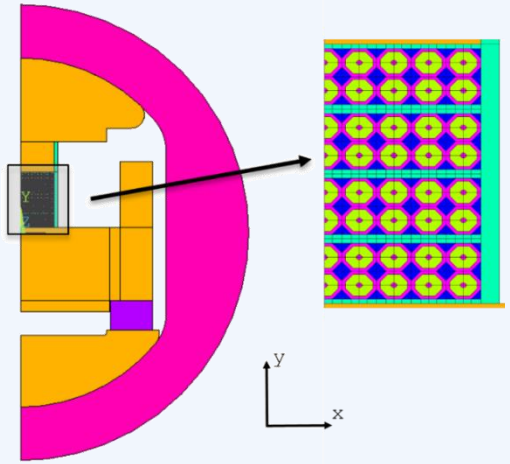

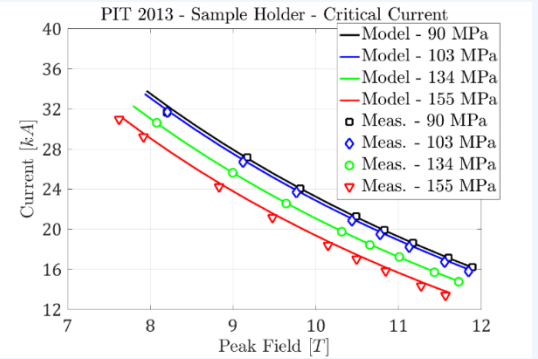

Vallone, Ferracin, Bordini et al.

Electro-mechanical limits on magnet configuration

A quick analogy, why is this important?

***Example!** C-WASP measurement for 0.85 mm RRP 108/127 15% rolled*

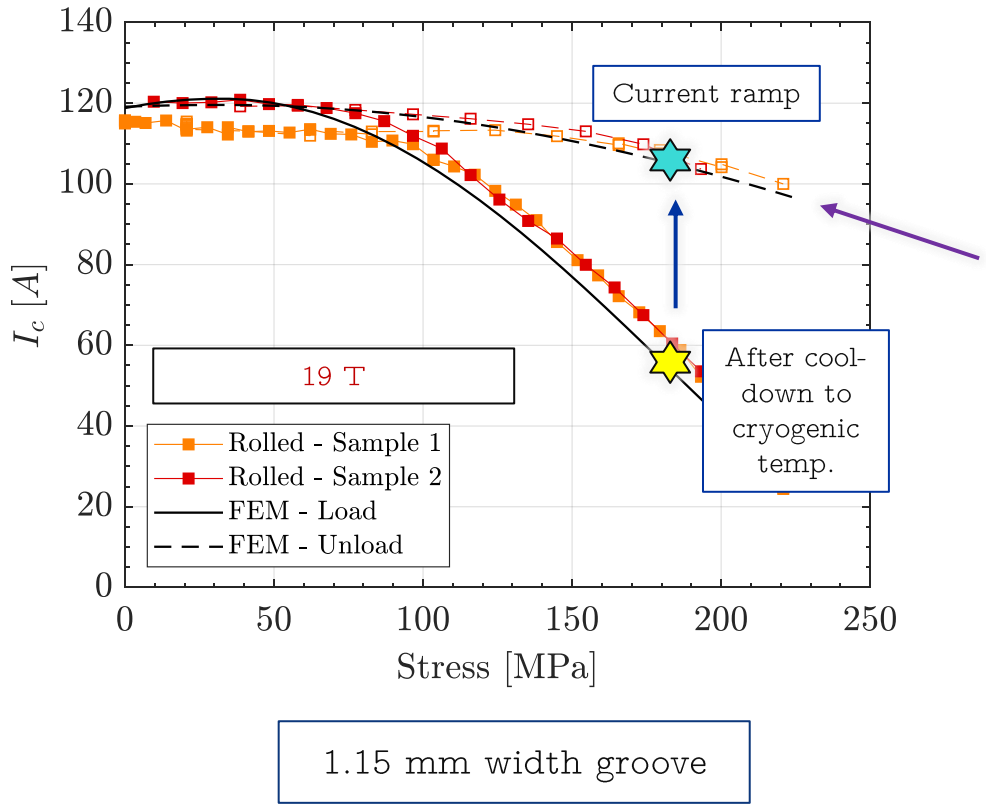

1.15 mm width groove

For the simulated magnet case - 4.5 K

In our peak field region, we follow the unload curve, whose slope is significantly lower than the load one!

This is an interesting feature of a magnet design, allowing to contain the decrease in quench current under reasonable limits for high stress levels (without decreasing the overall current density).

Correlation between strand and magnet results

- In the domain of application for the scaling law (no cracks), the conductor results could be correlated with the magnet ones when:

  1) The field dependence is considered
  2) The test configuration is such that is representative of the magnet one:

     - ❖ Strand / insulation / groove ratios consistent with the final cable ones

       Defines the fraction of force reaching the strand in the C-WASP experiment.

     - ❖ Support conditions are adequate (4-wall configuration, strain conditions)

Essential to consider all these factors in order to obtain meaningful information from strand / cable tests !

Magnet strand model:
Location of the quenching strand
Strain / stress state
Support conditions

The "measurable" (experimentally) is the transverse pre-load value.

C-WASP strand model:
Strain / stress state
Support conditions

The "measurable" (experimentally) is the normal applied stress value.

→ Consistent? Domain of application of the scaling law?

Correlation between both results. Conductor data to magnet application!

Ic vs. transverse stress on single wires

UNIVERSITÉ DE GENÈVE

Fitting parameters extracted from Ic vs axial strain measurements.

Simulation and experimental results:

0.85 mm RRP 108/127 15% rolled (HL-LHC MQXF quadrupole)

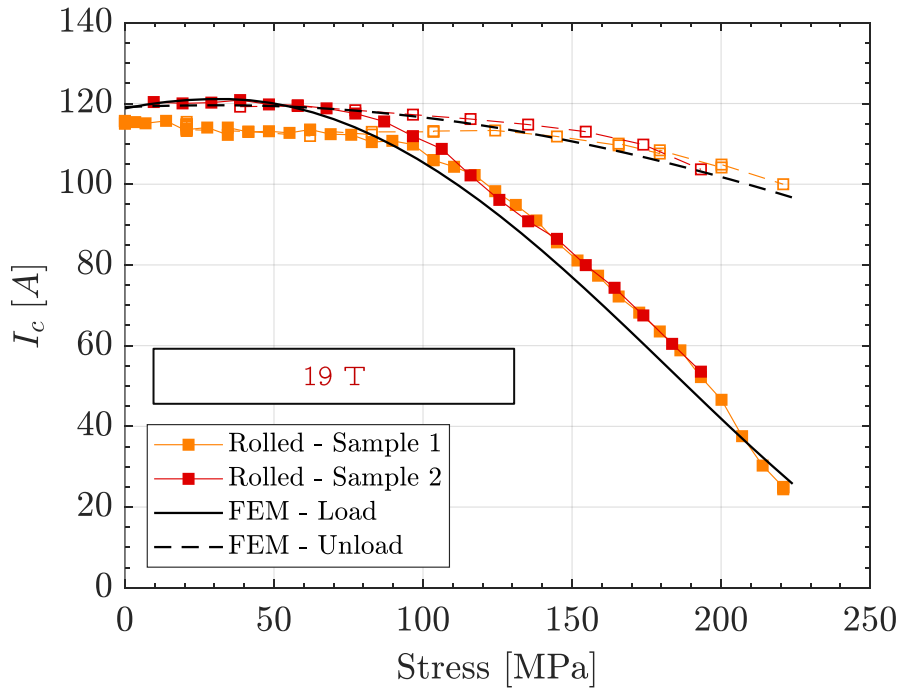

1.15 mm width groove

1 mm PIT 192 15% rolled (FRESCA2 dipole)

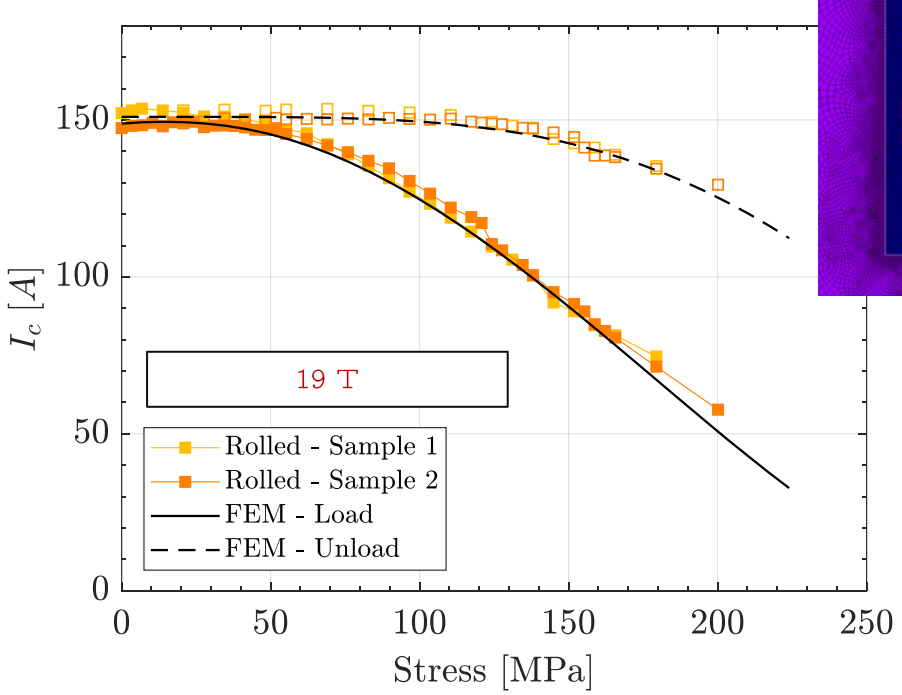

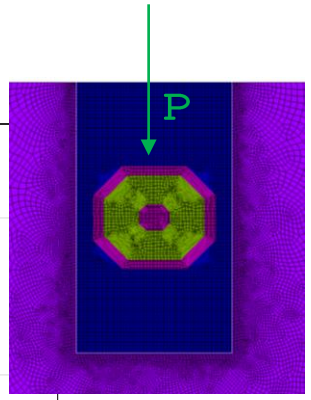

1.15 mm width groove

Ic vs. transverse stress on single wires

UNIVERSITÉ DE GENÈVE

Fitting parameters extracted from Ic vs axial strain measurements.

Simulation and experimental results:

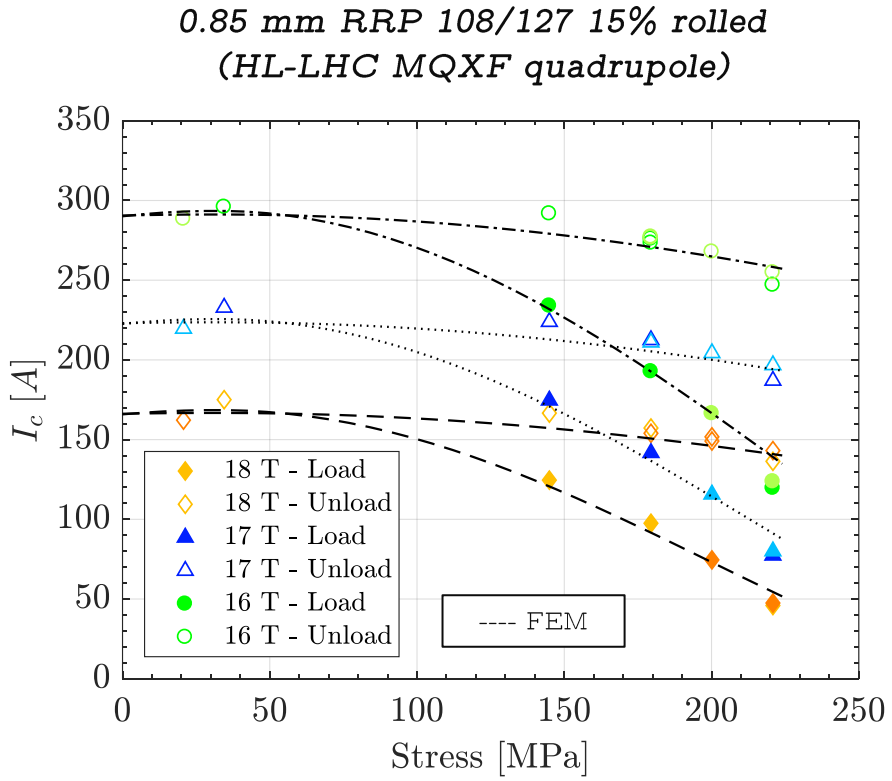

Permanent effect based on experimental data

Under the assumption of no cracks, we can use our Tc0, Bc20, C0 obtained from the axial test and map a "experimental" strain function from the measurements at 19 T

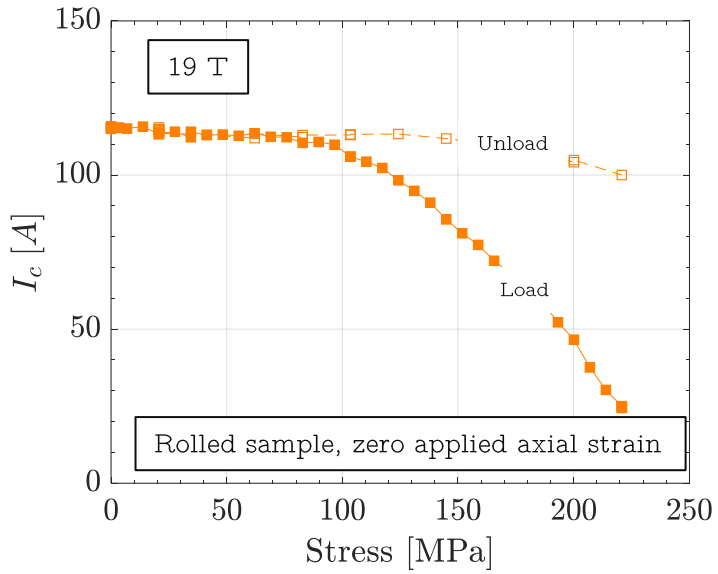

Assuming Tc0, Bc20, C0 from axial WASP

Optimization algorithm

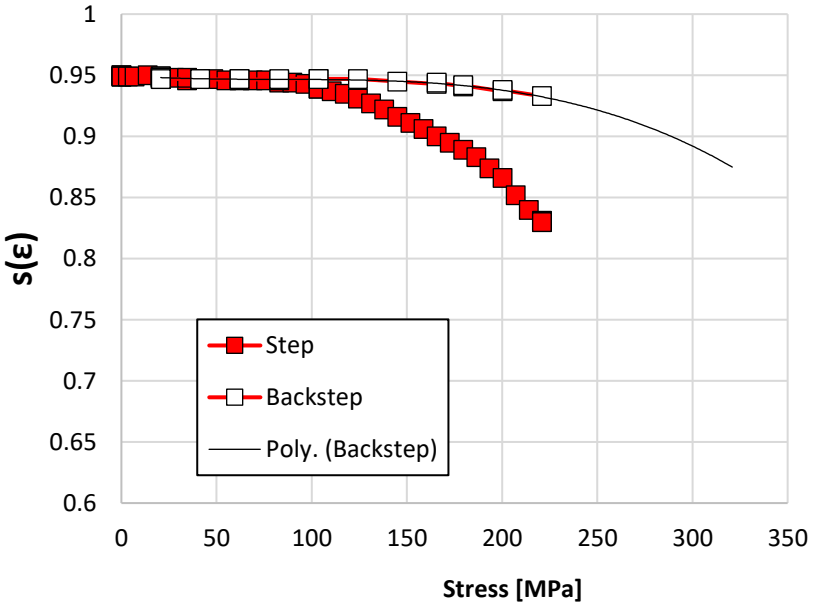

Permanent effect based on experimental data

Knowing the strain function (from measurements at 19T) and using the fitting parameters from the axial WASP we can compute Ic at any field, or Bc2 at any stress.

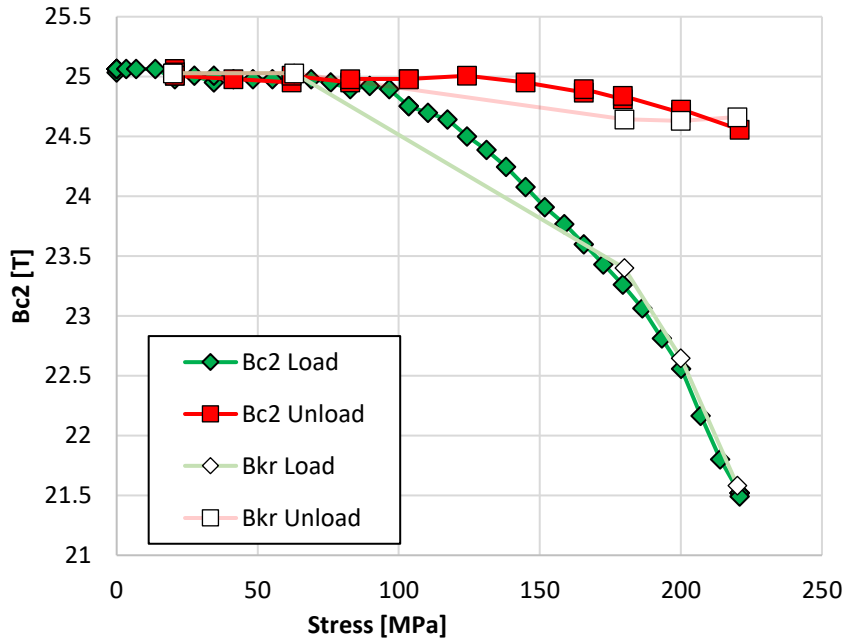

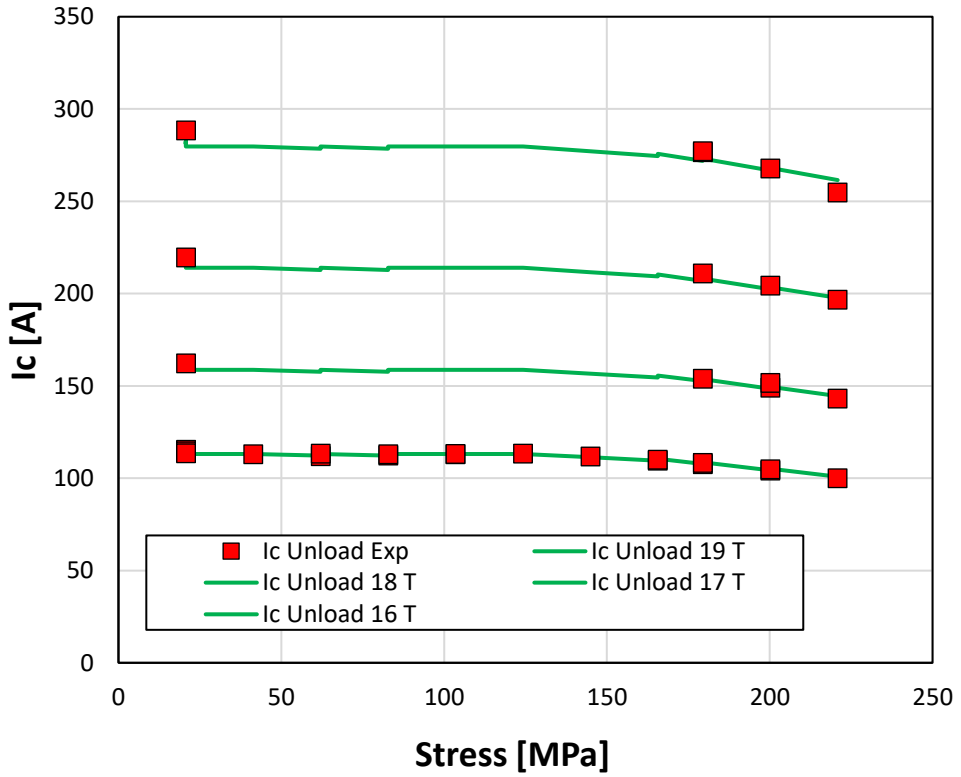

Permanent effect based on experimental data

Knowing the strain function (from measurements at 19T) and using the fitting parameters from the axial WASP we can compute Ic at any field, or Bc2 at any stress.

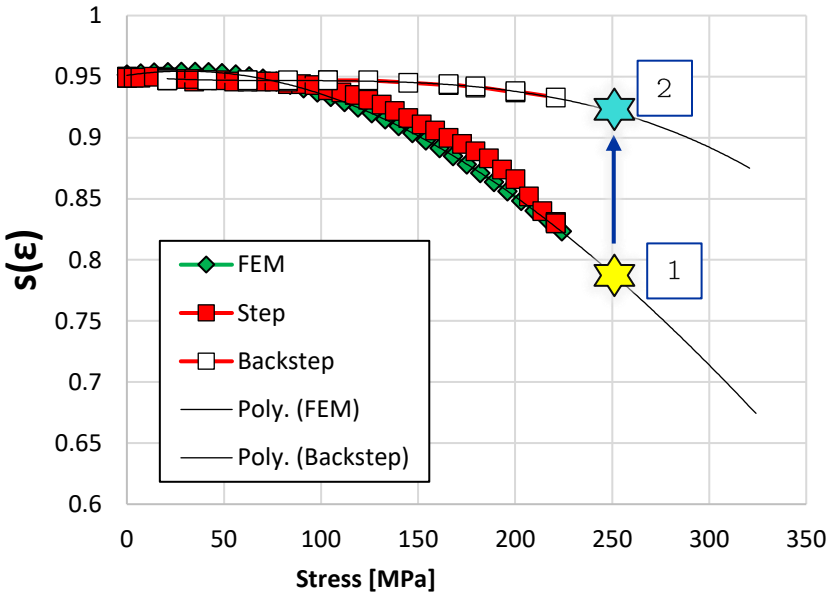

Furthermore, we know that our FEM matches well the part under load. To infer the Ic after unload, a simplistic approach could be to use the experimental strain function plot to determine s(ε) for the unloaded sample.

Note.- If our model would catch better the residual strain, this would not be needed.

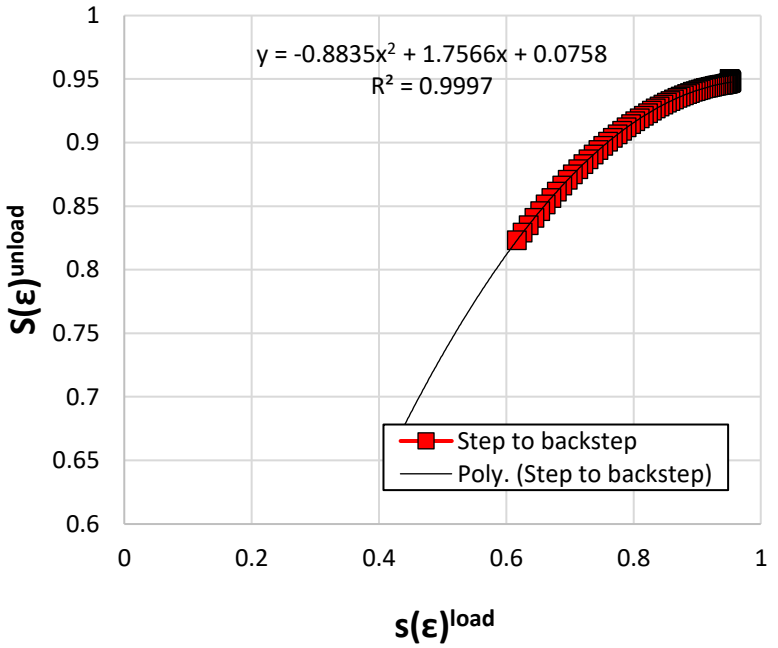

Thus, we can set our transfer function between $s(\varepsilon)^{load}$ and $s(\varepsilon)^{unload}$ based on UNIGE measurements.

Electro-mechanical limits on magnet configuration

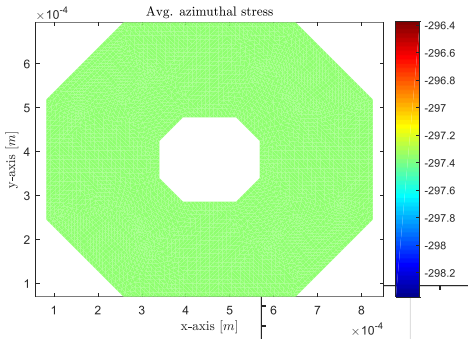

0.85 mm RRP 108/127 15% rolled (HL-LHC MQXF quadrupole)

1.15 mm width groove

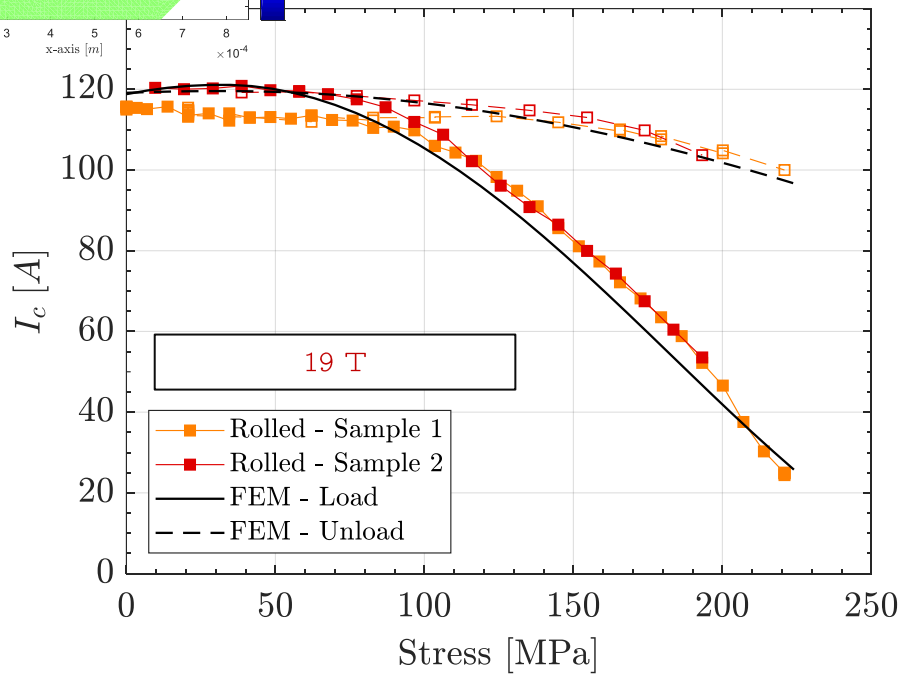

0.98 mm width groove

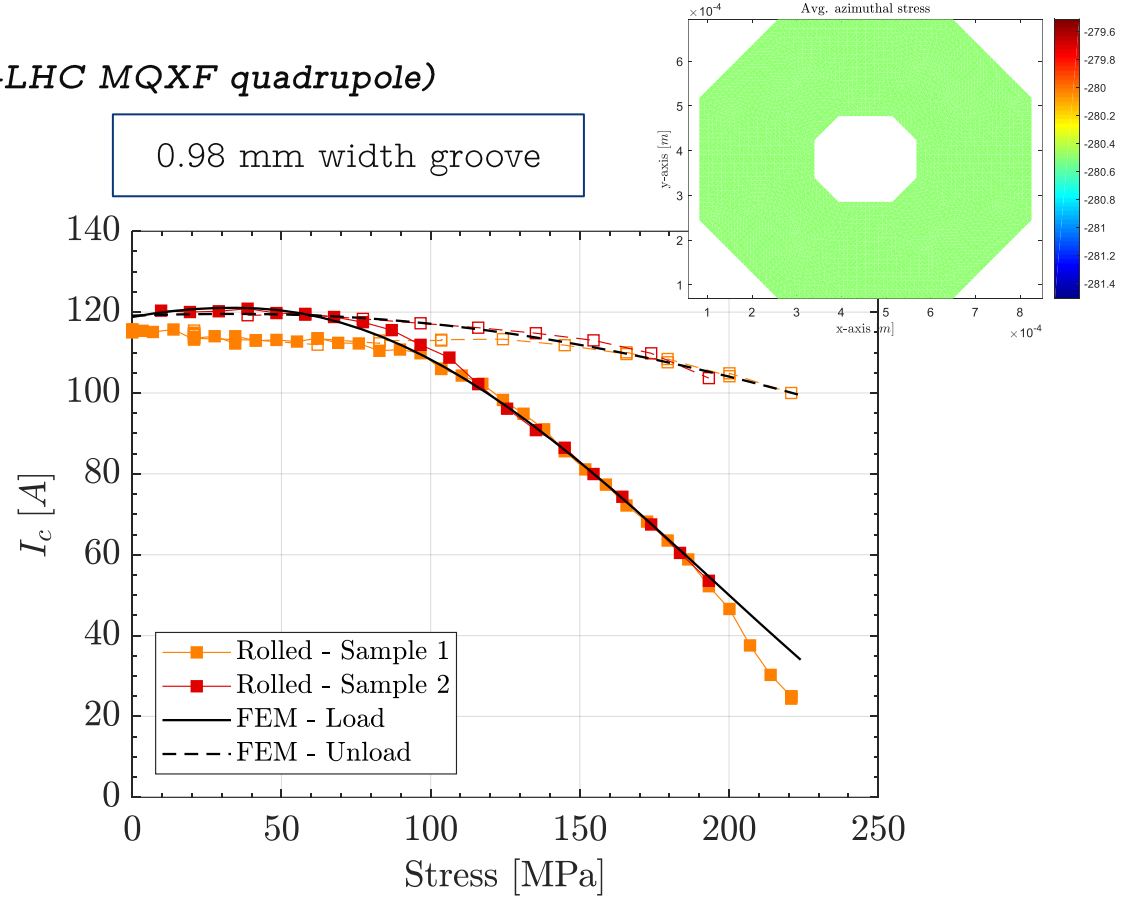

Setting the pressure, the total force in the system is larger for larger grooves (larger total force).

For the same groove and pressure (same total force), the force reaching the strand is larger for larger diameters.

Force fraction between UNIGE tests varies within 10%. See [5].

Magnet strand model

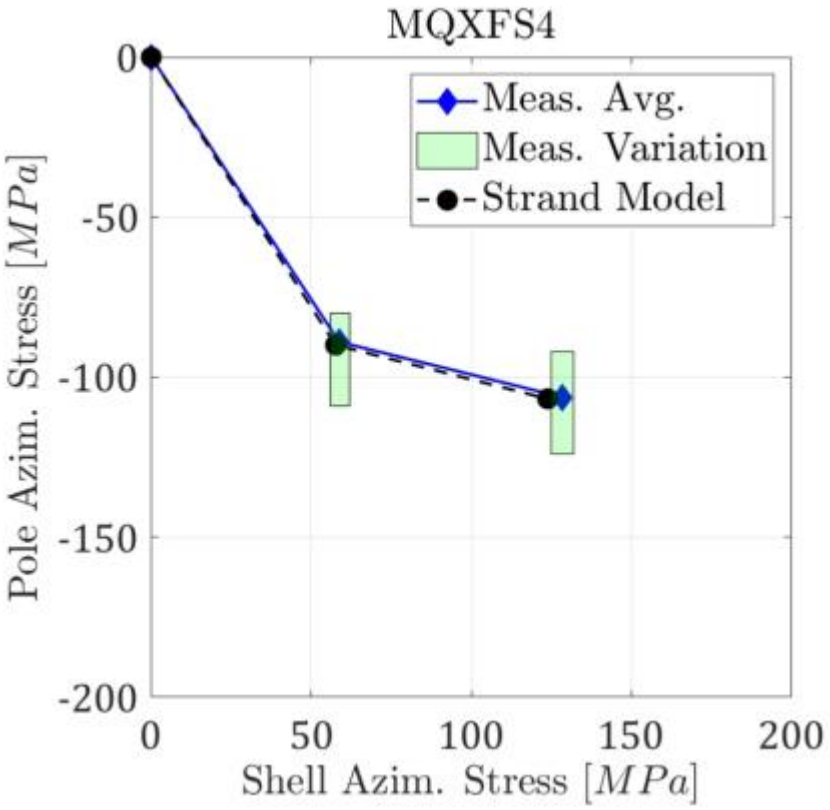

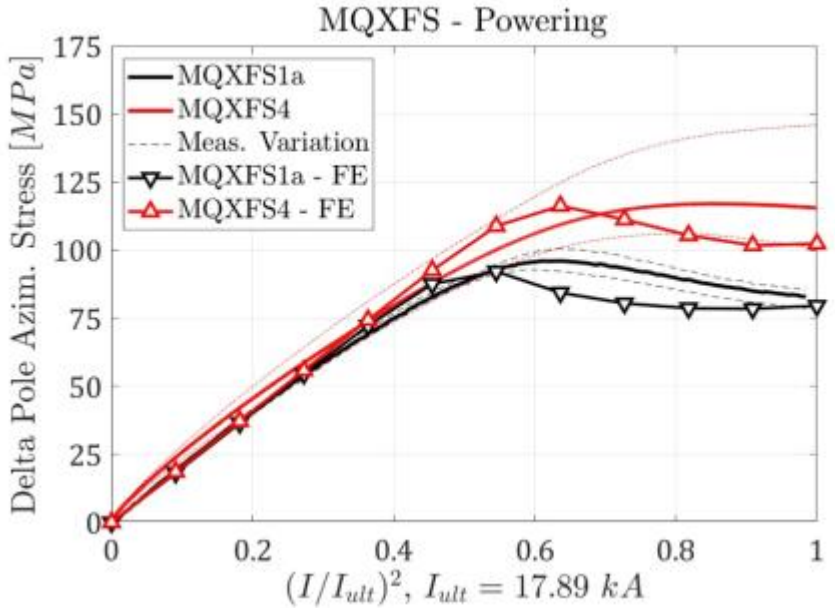

Vallone et al.

Correlation between strand and magnet results

- Average normal stress in the Nb_3Sn region (magnet model) after cool-down to cryogenic temperature.

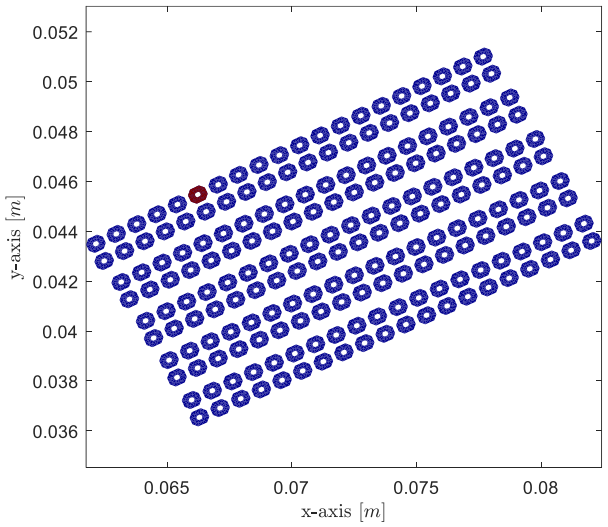

200 MPa pre-load – magnet model (1.9 K)

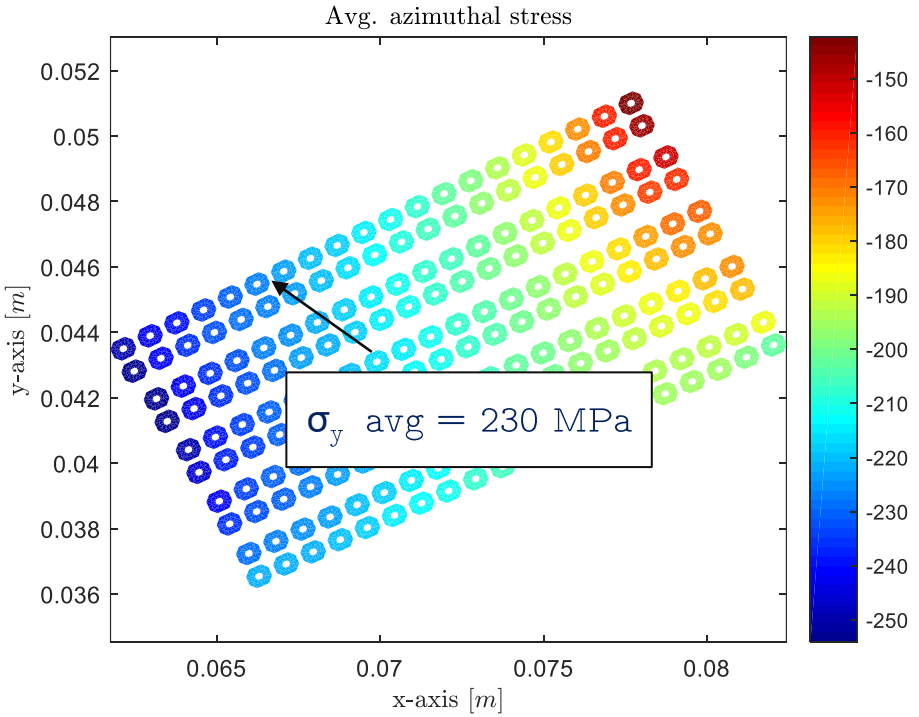

Electro-mechanical limits on magnet configuration

Magnet stress state:

***Reference pre-load** (4.5 K - Nb_3Sn region)*

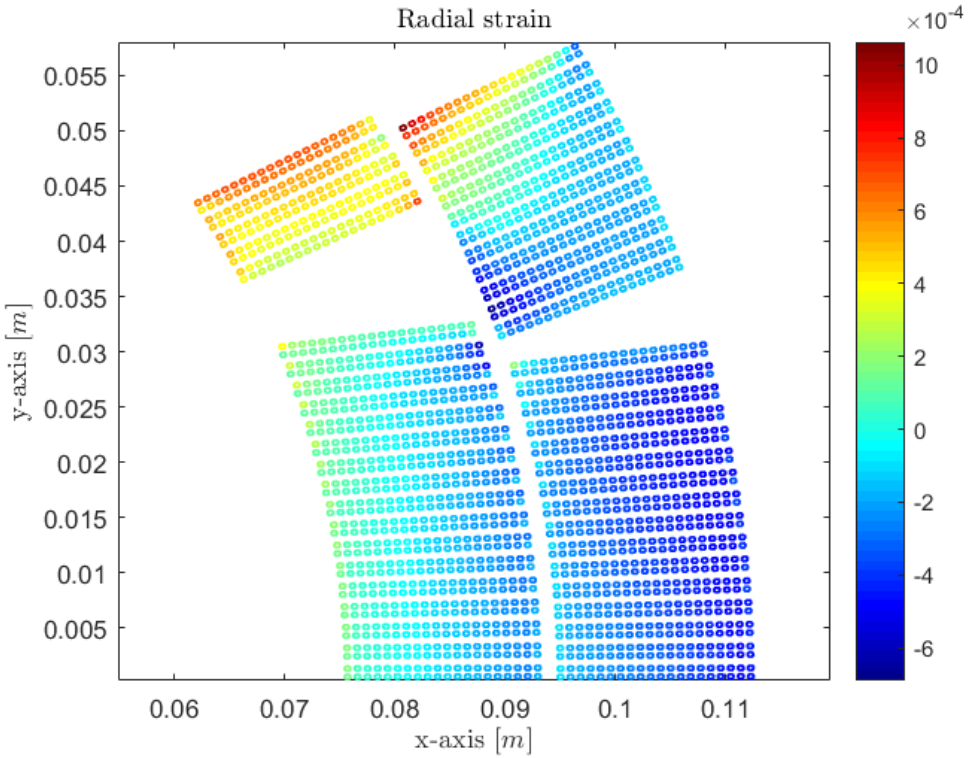

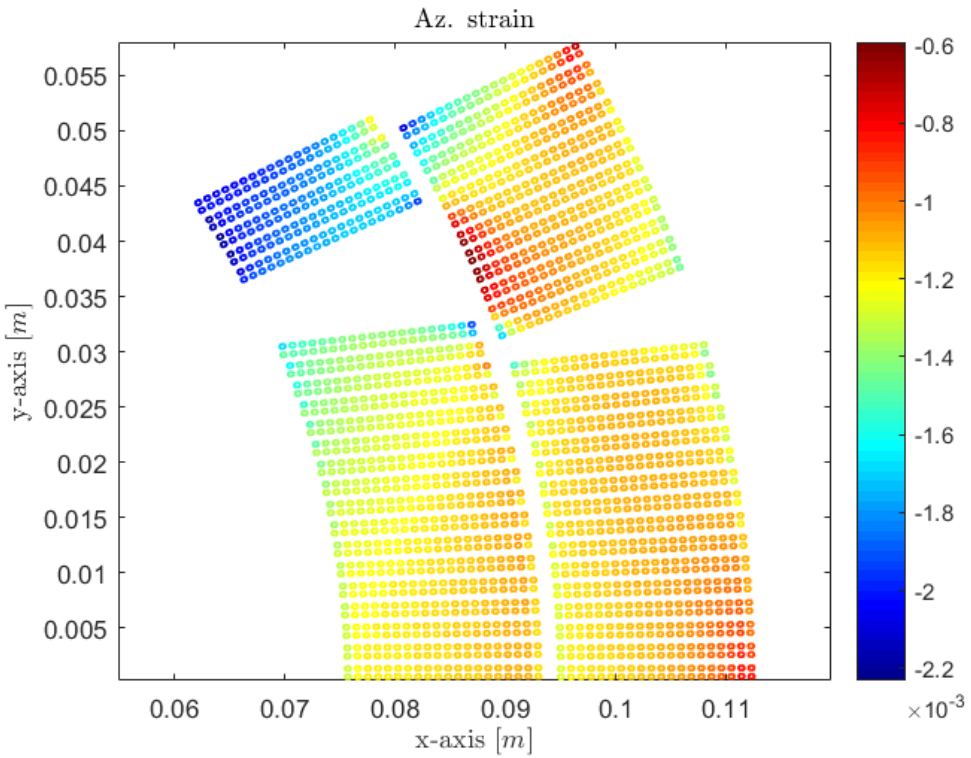

Azimuthal, radial and axial directions ~ principal.
Dominated by the azimuthal component.

Permanent effect based on experimental data.

Fixed temperature simplification:

$$J_c(B,\varepsilon) = C^* \left(\frac{B}{B^*_{c2}(\varepsilon)}\right)^{p-1} \left[1 - \left(\frac{B}{B^*_{c2}(\varepsilon)}\right)\right]^q$$

This is valid when the Ic reduction is governed by the lattice deformation (strain, no cracks) and far from Tc.

Since in our experiment at UNIGE we have found that no cracks are present in the wires (by inspection and by consistency in Bc2 decrease), we can use the expression above.

- Bc2(**ε**) is obtained by Kramer extrapolation* from the different field sweeps.
- One can then compute Ic at any magnetic field and any strain, if we know Bc2(**ε**).
- The same applies when the load is removed, there the permanent effect comes from $Bc2^{unload}$(**ε**).
- Using the expression we can get the permanent reduction by using: Ic^{unload}(**ε**)/ Ic0 [as a function of $Bc2^{unload}$(**ε**) and $Bc2^{unload}$(0)]
- Very interestingly for us, we can also get the ratio Ic^{unload}(**ε**)/ Ic^{load}(**ε**). In this case as a function of $Bc2^{unload}$(**ε**)/$Bc2^{load}$(**ε**).

With p=0.5 and q=2:

$$\frac{I_c^{unload}}{I_c^{load}}(B,\sigma) = \left[\frac{B_{c2}^{load}(\sigma)}{B_{c2}^{unload}(\sigma)}\right]^{3/2} - \left[\frac{B_{c2}^{unload}(\sigma) - B}{B_{c2}^{load}(\sigma) - B}\right]^2$$

$$\frac{I_c^{unload}(B,\sigma)}{I_{c0}\,(B,\sigma=0)} = \left[\frac{B_{c2}(0)}{B_{c2}^{unload}(\sigma)}\right]^{3/2} - \left[\frac{B_{c2}^{unload}(\sigma) - B}{B_{c2}(0) - B}\right]^2$$

C. Seagal et al. , "Evidence of Kramer extrapolation inaccuracy for predicting high field Nb_3Sn properties"
doi:10.1088/1742-6596/1559/1/012062

Permanent effect based on experimental data.

Results

Measured Ic and computed using Bc2(ε) after force unload agrees well.

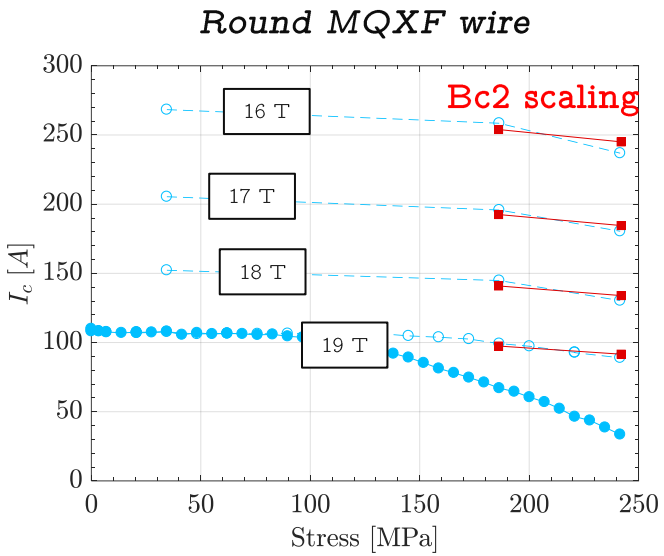

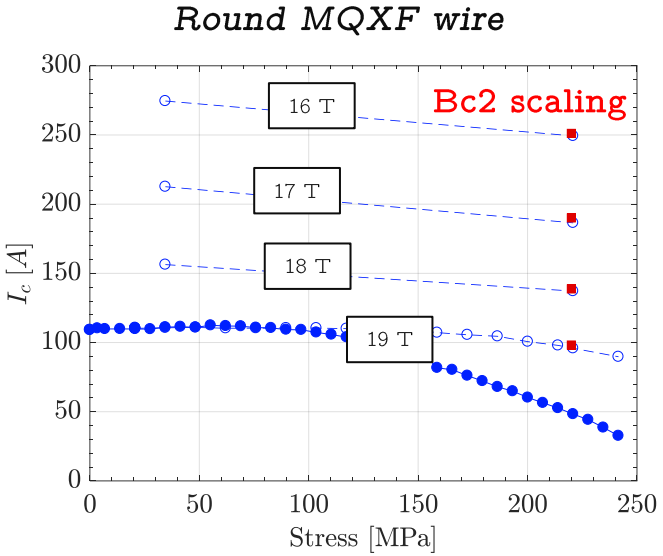

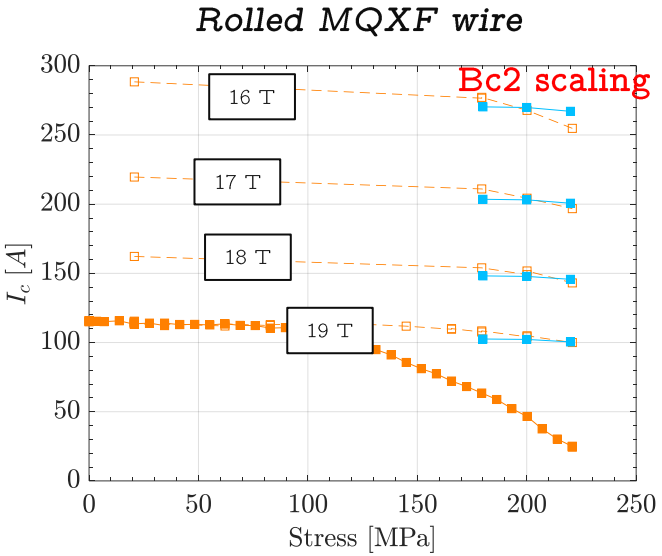

C. Seagal et al. , "Evidence of Kramer extrapolation inaccuracy for predicting high field Nb_3Sn properties"
doi:10.1088/1742-6596/1559/1/012062

References

[1] J. W. Ekin, “Effect of transverse compressive stress on the critical current and upper critical field of Nb3Sn,” J. Appl. Phys., vol. 62, no. 12, pp. 4829–4834, 1987.

[2] J. W. Ekin, Experimental Techniques for Low-Temperature Measurements: Cryostat Design, Material Properties, and Superconductor Criticalcurrent Test- ing. New York: Oxford University Press, 2006.

[3] B. Seeber, A. Ferreira, V. Abächerli, T. Boutboul, L. Oberli, and R. Flükiger, “Transport properties up to 1000 A of Nb3Sn wires under transverse compressive stress,” IEEE Trans. Appl. Supercond., vol. 17, no. 2, pp. 2643–2646, Jun. 2007.

[4] G. Mondonico, "Analysis of electromechanical properties of A15 type superconducting wires submitted to high mechanical loads," PhD. Thesis (2013).

[5] C. Calzolaio et al., “Electro-mechanical properties of PIT Nb3Sn wires under transverse stress: Experimental results and FEM analysis,” Supercond. Sci. Tech nol., vol. 28, no. 5, pp. 1–11, 2015.

[6] L. Gamperle, et al., “Determination of the electromechanical limits under transverse stress of high-performance Nb3Sn Rutherford cables from a single-wire experiment,” Phys. Rev. Research 2, 013211 – Published 26 February (2020).

[7] J. Ferradas Troitino et al, "Effects of the initial axial strain state on the response to transverse stress of high-performance RRP Nb3Sn wires," Supercond. Sci. Technol., vol. 34, p. 035008, 2021.

[8] T. Bagni et al., "Machine learning applied to X-ray tomography as a new tool to analyze the voids in RRP Nb3Sn wires," Scientific Reports, vol. 11, p. 7767, 2021.

[9] T. Bagni et al., "Formation and propagation of cracks in RRP Nb3Sn wires studied by deep learning applied to x-ray tomography," Supercond. Sci. Technol. , vol. 35, p. 104003, 2022.

[10] T. Bagni et al., "Tomography analysis tool: an application for image analysis based on unsupervised machine learning," IOP SciNotes, vol. 3, p. 015201, 2022.

[11] C. Senatore et al., “Degradation of Ic due to residual stress in high performance Nb3Sn wires submitted to compressive transverse force”, Supercond. Sci. Technol., Accepted for publication.

[12] B. Bordini, P. Alknes, A. Ballarino, L. Bottura, and L. Oberli, Critical current measurements of high-Jc Nb3Sn Rutherford cables under transverse compression, IEEE Trans. Appl. Supercond. 24, 9501005 (2014).

References

[13] J.-E. Duvauchelle, B. Bordini, J. Fleiter, and A. Ballarino, Critical current measurements under transverse pressure of a Nb3Sn rutherford cable based on 1 mm RRP wires, IEEE Trans. Appl. Supercond. 28, 4802305 (2018).

[14] G. De Marzi et al., "On the mechanisms governing the critical current reduction in Nb3Sn Rutherford cables under transverse stress," Scientific Reports, vol. 11, p. 7369, 2021.

[15] P. Ebermann et al., "Influence of transverse stress exerted at room temperature on the superconducting properties of Nb3Sn wires," Supercond. Sci. Technol., vol. 32, p. 095010, 2019, doi: 10.1088/1361-6668/ab2e51.

[16] P. Ebermann et al., "Irreversible degradation of Nb3Sn Rutherford cables due to transverse compressive stress at room temperature", Supercond. Sci. Technol., vol. 31, (2018).

[17] H. H. J. ten Kate, H. W. Weijers, and J. M. van Oort, Critical current degradation in Nb3Sn cables under transverse pressure, IEEE Trans. Appl. Supercond. 3, 1334 (1993).

[18] P. Gao, "Transverse pressure effect on superconducting Nb3Sn Rutherford and ReBCO roebel cables for accelerator magnets," PhD. Thesis, University of Twente (2019).

[19] Cheggour, N., Stauffer, T.C., Starch, W. et al., "Implications of the strain irreversibility cliff on the fabrication of particle-accelerator magnets made of restacked-rod-process Nb3Sn wires," Sci Rep 9, 5466 (2019).

[20] Cheggour, N., Stauffer, T.C., Starch, W. et al., "Precipitous change of the irreversible strain limit with heat-treatment temperature in Nb3Sn wires made by the restacked-rod process," Sci Rep 8, 13048 (2018).

[21] N. Cheggour et al., "Influence of Ti and Ta doping on the irreversible strain limit of ternary Nb3Sn superconducting wires made by the restacked-rod process," Superconductor Science and Technology, vol. 23, no. 5, May 2010.

[22] E. Barzi, T. Wokas, and A. V. Zlobin, Sensitivity of Nb3Sn Rutherford-type cables to transverse pressure, IEEE Trans. Appl. Supercond. 15, 1541 (2005).

[23] E. Barzi, "A device to test critical current sensitivity of Nb3Sn cables to pressure," in Proc. AIP Conf. Proc., 2002, vol. 614, pp. 45–52.

[24] E. Barzi, D. Turrioni, and A. V. Zlobin, "Effect of transverse pressure on brittle superconductors," IEEE Trans. Appl. Supercond., vol. 18, no. 2, pp. 980–983, Jun. 2008.

References

[25] H. Felice et al, "Performance of a Nb_3Sn Quadrupole Under High Stress," IEEE Transactions on Applied Superconductivity (Volume: 21, Issue: 3, June 2011).

[26] H. Bajas et al, "Advanced Nb_3Sn Conductors Tested in Racetrack Coil Configuration for the 11T Dipole Project," IEEE TRANSACTIONS ON APPLIED SUPERCONDUCTIVITY, VOL. 28, NO. 4, JUNE 2018.

[27] J.C. Perez et al, "Performance of the Short Model Coils Wound With the CERN 11-T Nb_3Sn Conductor," IEEE TRANSACTIONS ON APPLIED SUPERCONDUCTIVITY, VOL. 25, NO. 3, JUNE 2015.

[28] S. Izquierdo Bermudez et al., "Performance of a MQXF Nb3Sn Quadrupole Magnet Under Different Stress Level," IEEE Transactions on Applied Superconductivity (Volume: 32, Issue: 6, September 2022).

[29] L. Bottura et al., "$Jc(B, T, \epsilon)$ Parameterization for the ITER Nb3Sn Production," IEEE Trans. Appl. Supercond., Vol. 19, No. 3, (2009).

[30] B. Bordini, P. Alknes, L. Bottura, L. Rossi, and D. Valentinis, "An exponential scaling law for the strain dependence of the Nb3Sn critical current density," Supercond. Sci. Technol., vol. 26, no. 7, 2013, Art. no. 075014.

[31] A. Cattabiani, D. Baffari, and B. Bordini, "A 3D finite element model of the reversible critical current reduction due to transverse load in Nb3Sn wires," IEEE Trans. Appl. Supercond., vol. 30, no. 4, Feb. 2020, Art. no. 8401006, doi: 10.1109/tasc.2020.2977038.

[32] D. Baffari et al., "Effect of the Sub-Elements Layout on the Electro-Mechanical Properties of High Jc Nb3Sn Wires Under Transverse Load: Numerical Simulations," IEEE Transactions on applied superconductivity Vol. 32, No. 6, September 2022.

[33] T. Wang, L. Chiesa, M. Takayasu, and B. Bordini, "A novel modeling to predict the critical current behavior of Nb3Sn PIT strand under transverse load based on a scaling law and finite element analysis," Cryogenics, vol. 63, pp. 275–281, 2014.

References

[34] G. Vallone, B. Bordini, and P. Ferracin, “Computation of the reversible critical current degradation in Nb3Sn rutherford cables for particle accelerator magnets,” IEEE Trans. Appl. Supercond., vol. 28, no. 4, Jun. 2018, Art. no. 4801506.

[35] G. Vallone, E. Anderssen, B. Bordini, P. Ferracin, J. F. Troitino, and S. Prestemon, “A methodology to compute the critical current limit in Nb3Sn magnets,” Superconductor Sci. Technol., 2020. [Online]. Available: https://doi.org/10.1088/1361-6668/abc56b